Université de Liège

ArGEnCo

Excavation damaged zone modelling with shear strain localisation in claystone

B. Pardoen - S. Levasseur - F. Collin - J.P. Radu

First International Workshop on the Finite Element Code LAGAMINE (LAGASHOP 2013)

9-12 September 2013

University of Liège, Opera Complex, Liège

Excavation damaged zone

*In situ* evidences :

Observations and measurements (ANDRA URL, GED Gallery, Armand *et al.* 2013, Cruchaudet *et al.* 2010b).

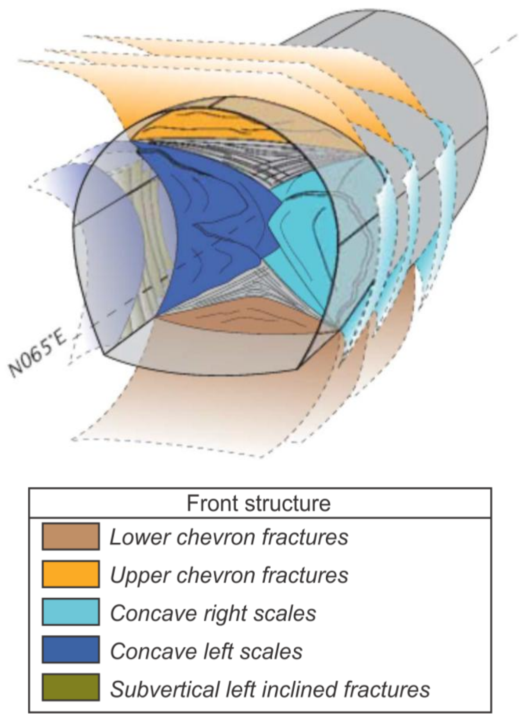

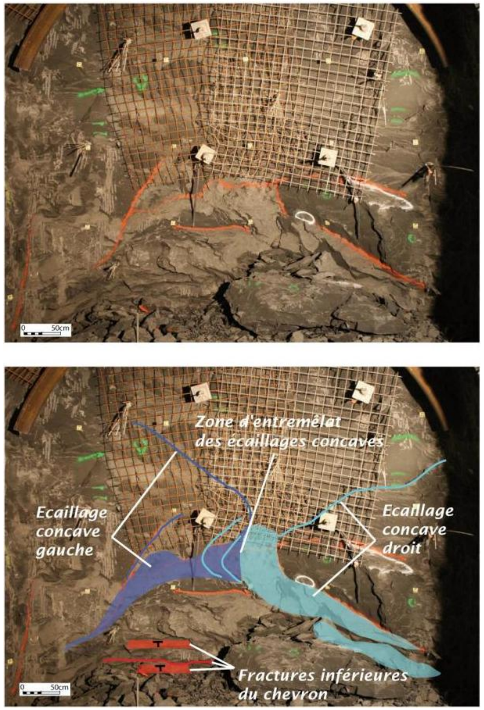

Front of the section GED1002

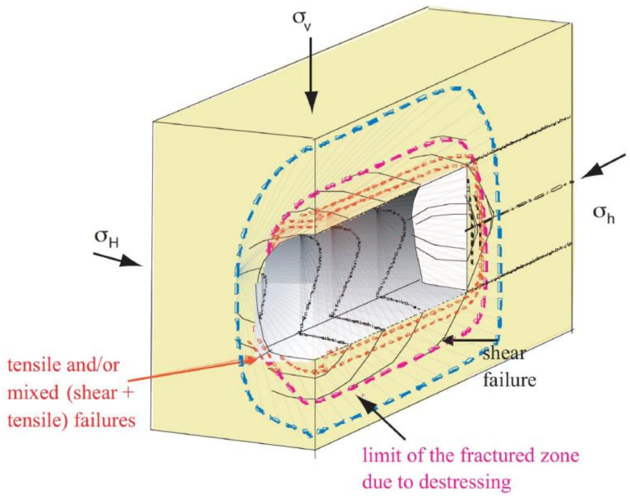

Shear and tension fractures (Bordeau *et al.* 2007)

Major issues : prediction of the <u>extension</u> and fracturing <u>structure</u>.

study - damaged zone development with shear strain localisation
- influence of the gallery ventilation and permeability variation.

Outline

1. CONSTITUTIVE MODELS
2. NUMERICAL RESULTS FOR GALLERY EXCAVATION
3. CONCLUSIONS AND OUTLOOKS

Outline

1. **CONSTITUTIVE MODELS**
2. NUMERICAL RESULTS FOR GALLERY EXCAVATION
3. CONCLUSIONS AND OUTLOOKS

Modelling of strain localisation – coupled 2^d gradient model : (Chambon *et al.*, 1998 and 2001)

Classical FE → mesh dependency → enriched model : 2d gradient

Porous media, multiphasic : solid + fluid

The continuum is enriched with microstructure effects. The kinematics include the classical one (macro) and the microkinematics (Toupin 1962, Mindlin 1964, Germain 1973, Collin et al., 2006).

Balance equations :

$$\int_{\Omega} \left(\sigma_{ij} \frac{\partial u_i^*}{\partial x_j} + \Sigma_{ijk} \frac{\partial^2 u_i^*}{\partial x_j \partial x_k} \right) d\Omega = \int_{\Omega} G_i u_i^* d\Omega + \int_{\Gamma_\sigma} \left(\bar{t}_i u_i^* + \bar{T}_i D u_i^* \right) d\Gamma$$

$$\int_{\Omega} \left(\frac{\partial M}{\partial t} p_w^* - m_i \frac{\partial p_w^*}{\partial x_i} \right) d\Omega = \int_{\Omega} Q \, p_w^* \, d\Omega + \int_{\Gamma_q} \bar{q} \, p_w^* \, d\Gamma$$

Σ_{ijk} is the double stress, which needs an additional constitutive law.

Modelling of strain localisation – coupled 2[d] gradient model :

- Solid and fluid phases behaviour :

Multiphasic medium under unsaturated condition (p_g=cst)

Compressibility of the solid grain skeleton.

Permeability : anisotropy and evolution with mechanical parameter

→ Bishop's stress definition : $\sigma_{ij} = \sigma'_{ij} - b\, S_{r,w}\, p_w\, \delta_{ij}$

Biot's coefficient : $b = 1 - \frac{K_0}{K_s}$

Fluid mass flow (advection, Darcy) : $m_{w,i} = -\rho_w \frac{k_{ij}\, k_{r,w}}{\mu_w} \left(\frac{\partial p_w}{\partial x_j} + \rho_w g_j \right)$

Modelling of strain localisation – coupled 2[d] gradient model :

- Solid and fluid phases behaviour :

Multiphasic medium under unsaturated condition (p_g=cst)

Compressibility of the solid grain skeleton.

Permeability : anisotropy and evolution with mechanical parameter

→ Bishop's stress definition : $\sigma_{ij} = \sigma'_{ij} - b\, S_{r,w}\, p_w\, \delta_{ij}$

Biot's coefficient : $b = 1 - \frac{K_0}{K_s}$

Fluid mass flow (advection, Darcy) : $m_{w,i} = -\rho_w \frac{k_{ij}\, k_{r,w}}{\mu_w}\left(\frac{\partial p_w}{\partial x_j} + \rho_w g_j\right)$

- Stiffness matrix :

$$[E^t]_{25\times25} = \begin{bmatrix} E^t_{1_{4\times4}} & 0_{4\times2} & \boxed{K^t_{WM_{4\times3}}} & 0_{4\times8} & 0_{4\times4} & -I_{4\times4} \\ G^t_{1_{2\times4}} & 0_{2\times2} & G^t_{2_{2\times3}} & 0_{2\times8} & 0_{2\times4} & 0_{2\times4} \\ \boxed{K^t_{MW_{3\times4}}} & 0_{3\times2} & \boxed{K^t_{WW_{3\times3}}} & 0_{3\times8} & 0_{3\times4} & 0_{3\times4} \\ E^t_{2_{8\times4}} & 0_{8\times2} & 0_{8\times3} & D^t_{8\times8} & 0_{8\times4} & 0_{8\times4} \\ E^t_{3_{4\times4}} & 0_{4\times2} & 0_{4\times3} & 0_{4\times8} & 0_{4\times4} & I_{4\times4} \\ E^t_{4_{4\times4}} & 0_{4\times2} & 0_{4\times3} & 0_{4\times8} & -I_{4\times4} & 0_{4\times4} \end{bmatrix}$$

Mechanical model – 1st gradient model :

Non-associated elasto-plastic internal friction model,
with a Drucker-Prager yield surface :

$$F \equiv II_{\hat{\sigma}} - m\left(I_{\sigma} + \frac{3c}{\tan\phi_C} \right) = 0$$

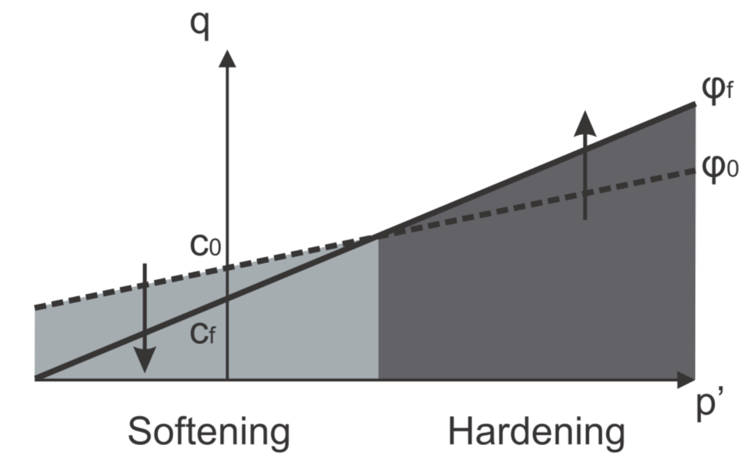

Hardening of φ and softening c as a function
of the Von Mises equivalent plastic strain ε^p_{eq} :

$$\varepsilon^p_{eq} = \sqrt{\frac{2}{3}\hat{\varepsilon}^p_{ij}\hat{\varepsilon}^p_{ij}}$$

$$\phi_C = \phi_{C0} + \frac{\left(\phi_{Cf} - \phi_{C0}\right)\varepsilon^p_{eq}}{B_\phi + \varepsilon^p_{eq}}$$

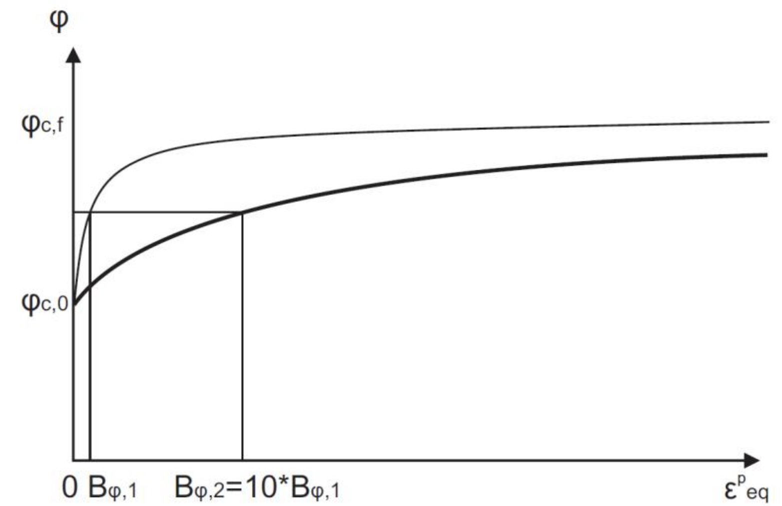

<u>Mechanical model – 2^d gradient model :</u> (Chambon *et al.*, 1998 and 2001)

Double stress Σ_{ijk} additional constitutive law : linear elastic law (Mindlin, 1964) function of the (micro) second gradient of displacement field u_i , $h_{ijk} = \dfrac{\partial v_{ij}}{\partial x_k} = \dfrac{\partial^2 u_i}{\partial x_j \partial x_k}$:

$$\begin{bmatrix} \tilde{\Sigma}_{111} \\ \tilde{\Sigma}_{112} \\ \tilde{\Sigma}_{121} \\ \tilde{\Sigma}_{122} \\ \tilde{\Sigma}_{211} \\ \tilde{\Sigma}_{212} \\ \tilde{\Sigma}_{221} \\ \tilde{\Sigma}_{222} \end{bmatrix} = \underline{D} \begin{bmatrix} 1 & 0 & 0 & 0 & 0 & \frac{1}{2} & \frac{1}{2} & 0 \\ 0 & \frac{1}{2} & \frac{1}{2} & 0 & -\frac{1}{2} & 0 & 0 & \frac{1}{2} \\ 0 & \frac{1}{2} & \frac{1}{2} & 0 & -\frac{1}{2} & 0 & 0 & \frac{1}{2} \\ 0 & 0 & 0 & 1 & 0 & -\frac{1}{2} & -\frac{1}{2} & 0 \\ 0 & -\frac{1}{2} & -\frac{1}{2} & 0 & 1 & 0 & 0 & 0 \\ \frac{1}{2} & 0 & 0 & -\frac{1}{2} & 0 & \frac{1}{2} & \frac{1}{2} & 0 \\ \frac{1}{2} & 0 & 0 & -\frac{1}{2} & 0 & \frac{1}{2} & \frac{1}{2} & 0 \\ 0 & \frac{1}{2} & \frac{1}{2} & 0 & 0 & 0 & 0 & 0 \end{bmatrix} \begin{bmatrix} \frac{\partial \dot{v}_{11}}{\partial x_1} \\ \frac{\partial \dot{v}_{11}}{\partial x_2} \\ \frac{\partial \dot{v}_{12}}{\partial x_1} \\ \frac{\partial \dot{v}_{12}}{\partial x_2} \\ \frac{\partial \dot{v}_{21}}{\partial x_1} \\ \frac{\partial \dot{v}_{21}}{\partial x_2} \\ \frac{\partial \dot{v}_{22}}{\partial x_1} \\ \frac{\partial \dot{v}_{22}}{\partial x_2} \end{bmatrix}$$

It depends only on one elastic parameter D. The shear band width is proportional to this parameter.
(Chambon *et al.,* 1998, Kotronis *et al.*, 2007).

Fluid phase :

Water retention and permeability curves (Van Genuchten's model) :

$$S_{r,w} = S_{res} + \left(S_{\max} - S_{res}\right)\left[1 + \left(\frac{p_c}{P_r}\right)^N\right]^{-M}$$

$$k_{r,w} = \sqrt{S_{r,w}}\left[1 - \left(1 - S_{r,w}^{1/M}\right)^M\right]^2$$

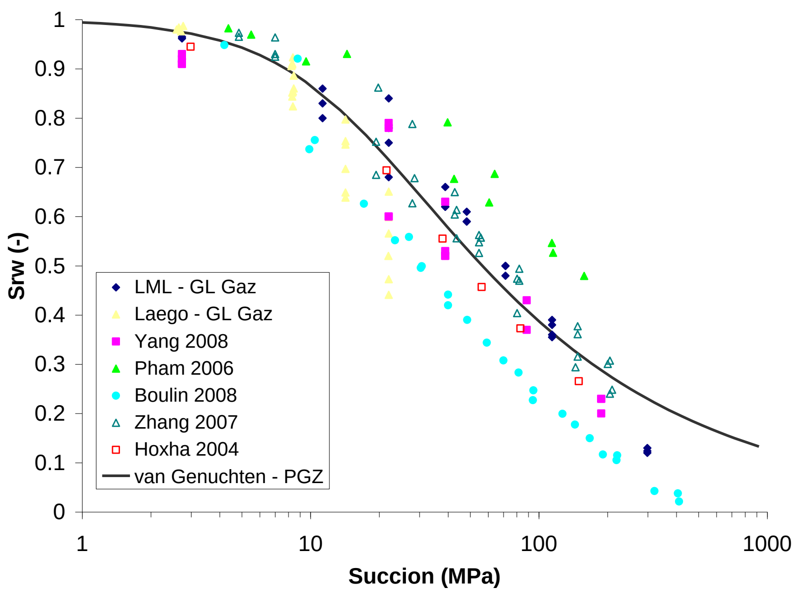

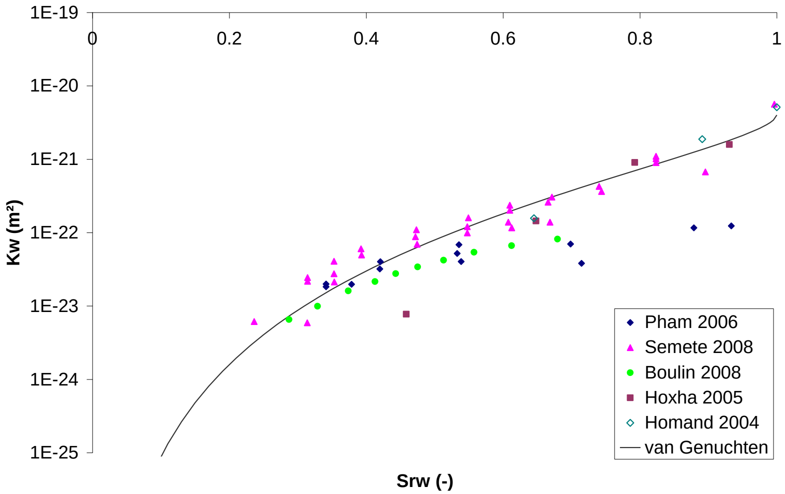

Outline

1. CONSTITUTIVE MODELS

2. NUMERICAL RESULTS FOR GALLERY EXCAVATION

- **2D : ventilation, permeability variation**

- 3D

3. CONCLUSIONS AND OUTLOOKS

Full gallery :

Modelling of a full gallery to avoid symmetry assumption.

HM modelling in 2D plane strain state.
Gallery radius = 2.3 m.

Anisotropy (Andra URL) :

→ hydraulic permeability anisotropy
$k_{hor/vert} = 4\ 10^{-20}\ /\ 1.33\ 10^{-20}$ [m²]

→ initial anisotropic stress state
$p_{w,0} = 4.5$ [Mpa]
$\sigma_{y,0} = \sigma_{z,0} = 12$ [Mpa]
$\sigma_{x,0} = 15.6$ [MPa]

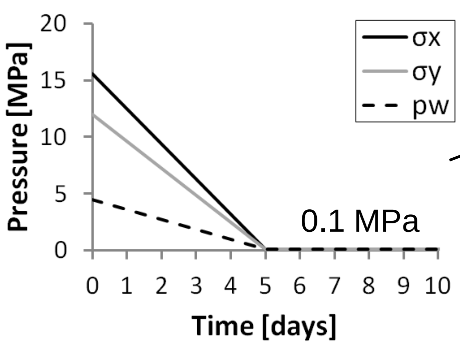

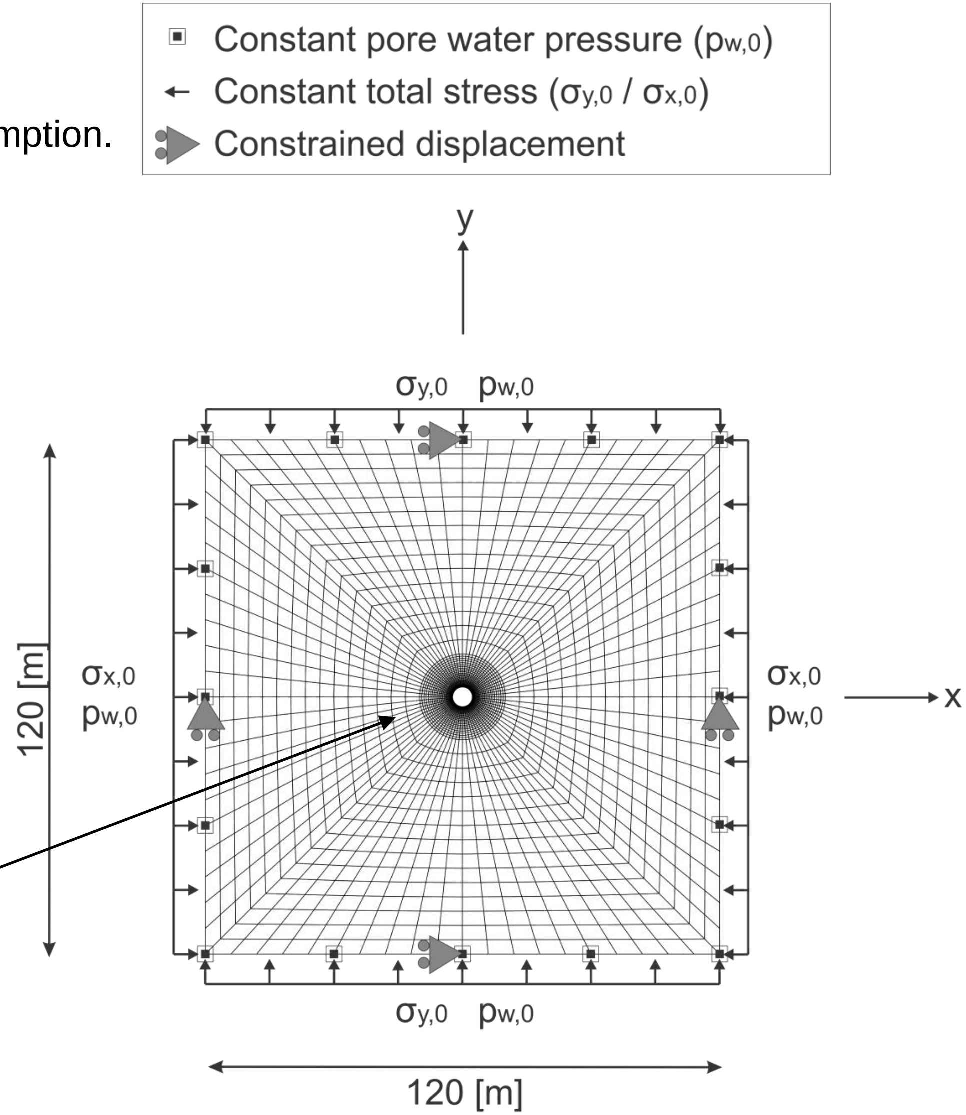

Localisation zone :

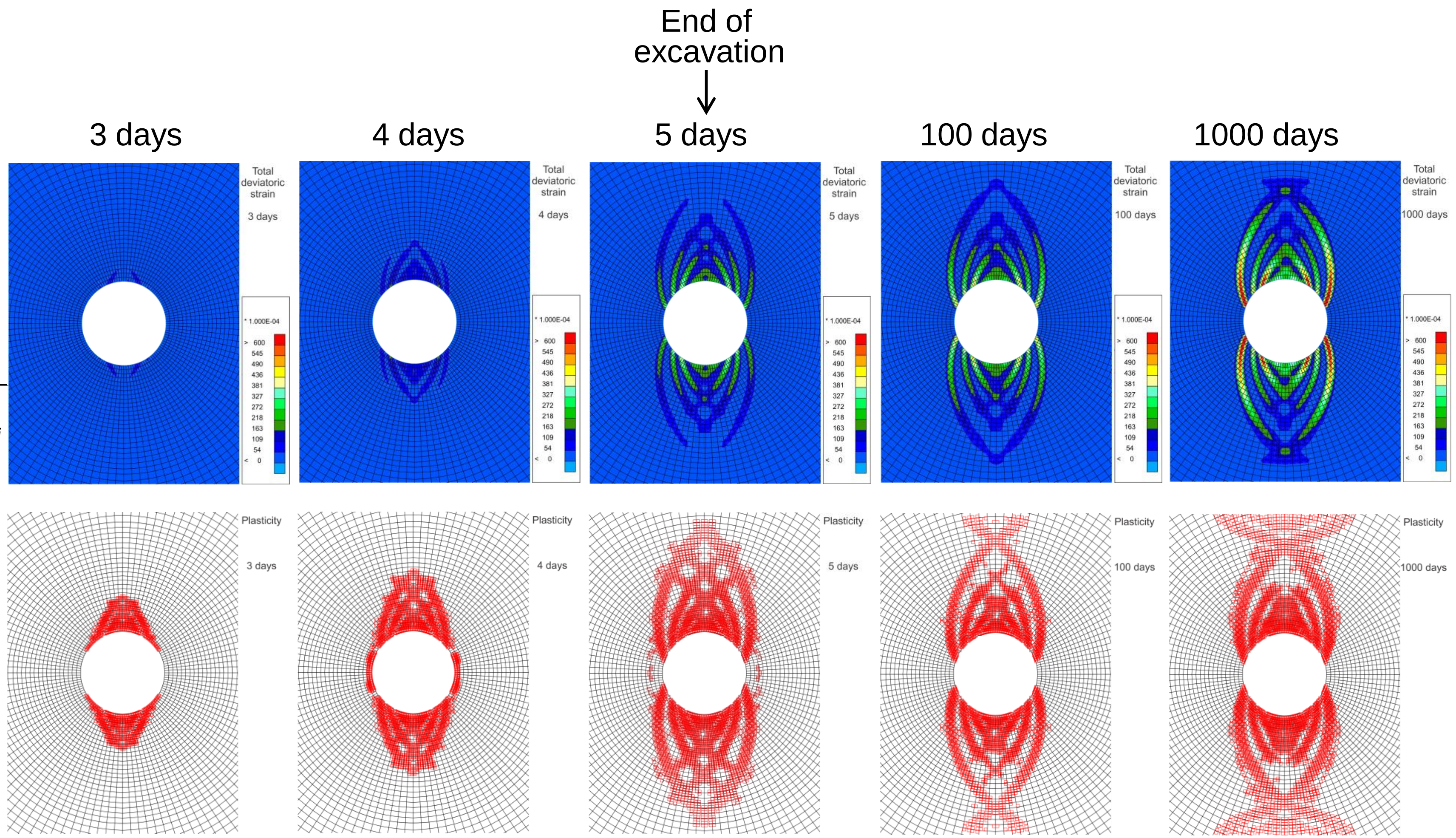

Total deviatoric strain

$$\varepsilon_{eq} = \sqrt{\frac{2}{3}\hat{\varepsilon}_{ij}\hat{\varepsilon}_{ij}}$$

Plasticity

<u>Localisation zone :</u>

Chevron fracture : - pattern corresponding to *in situ* observations (Armand *et al.* 2013).

- concentrated above the gallery because of the anisotropic stress state.

The extension of the excavation damaged zone obtained numerically corresponds fairly well to the *in situ* experimental measurements of shear fractures.

Numerical result
Shear strain localisation

Symmetry

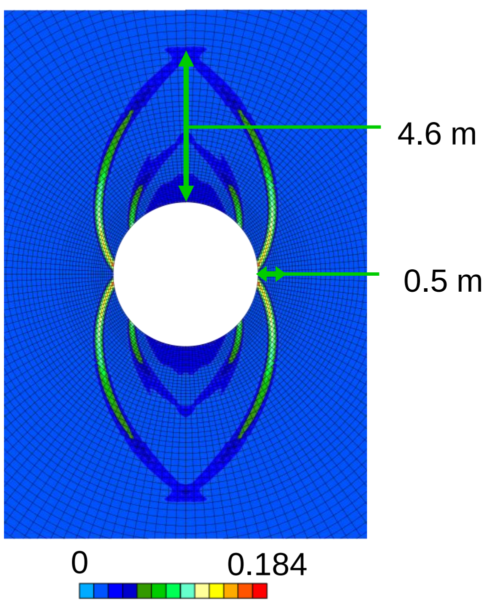

In situ
Shear fractures

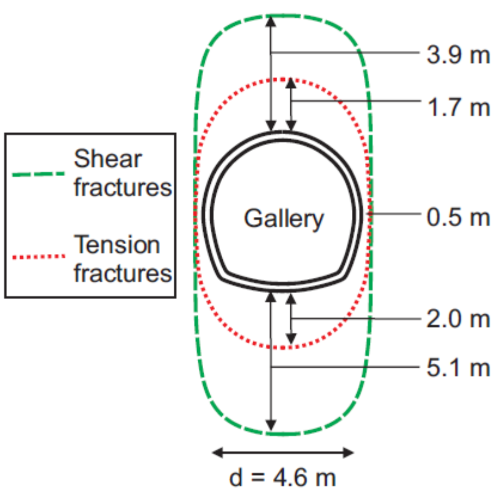

2. Numerical results for gallery excavation – 2D

Quarter of gallery :

By symmetry: quarter of the gallery

Second gradient boundary condition (Zervos et al. 2001)

Gradient terms in the equilibrium equations

→ Higher order constrains

→ Radial displacement must be symmetric on both sides of the symmetry axes

→ Normal derivative cancel

$$\frac{\partial u_x}{\partial y} = 0 \quad \text{along the x-axis}$$

$$\frac{\partial u_y}{\partial x} = 0 \quad \text{along the y-axis}$$

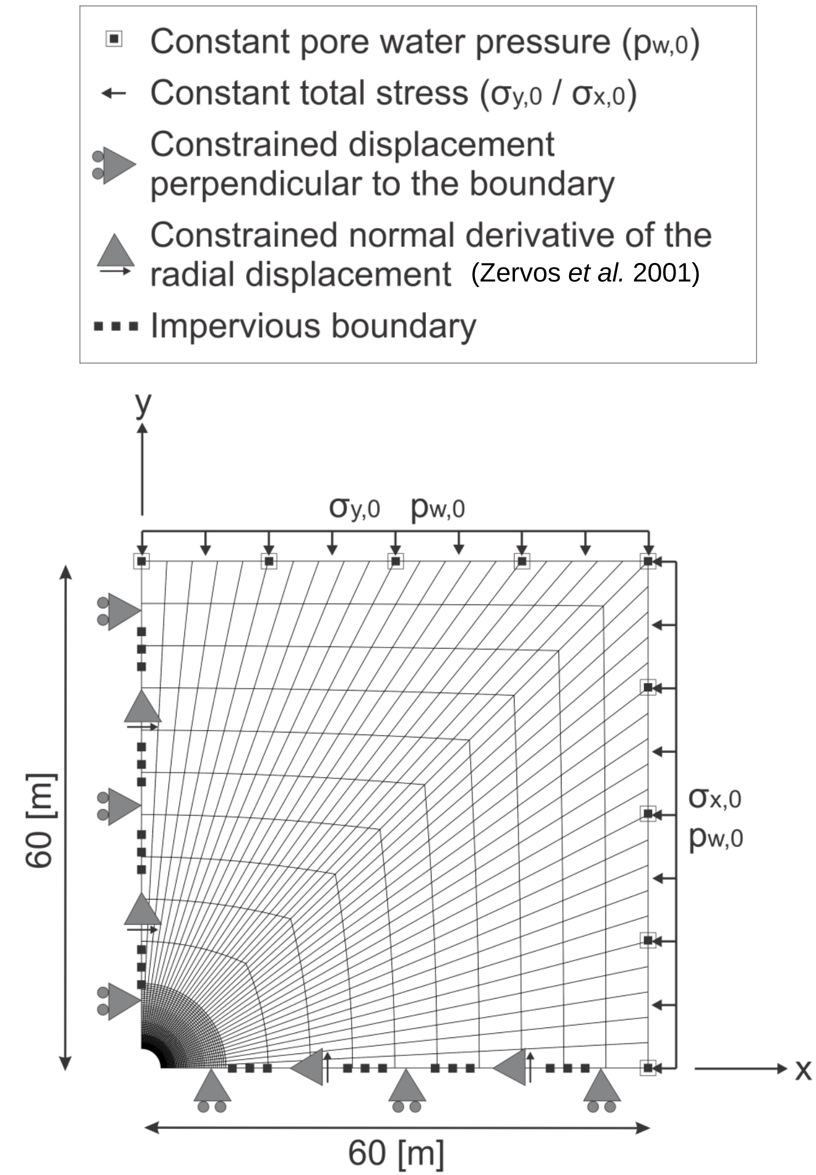

Influence of second gradient boundary condition :

End of the calculation

Full gallery

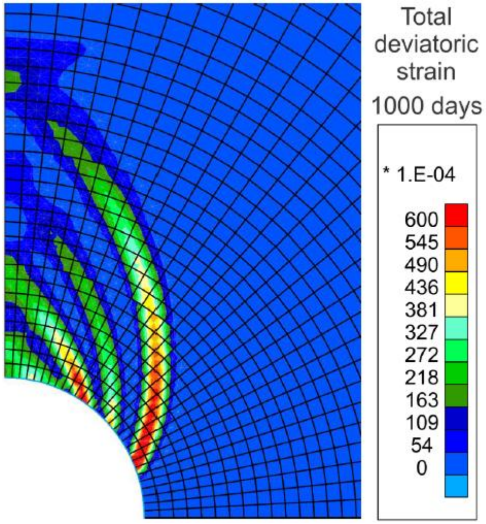

Quarter

with 2^d gradient BC

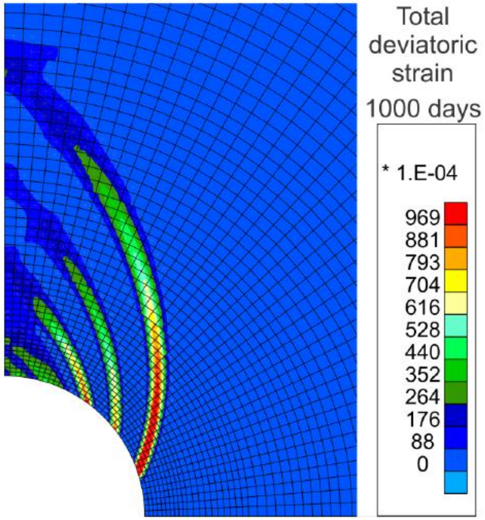

Quarter

without 2^d gradient BC

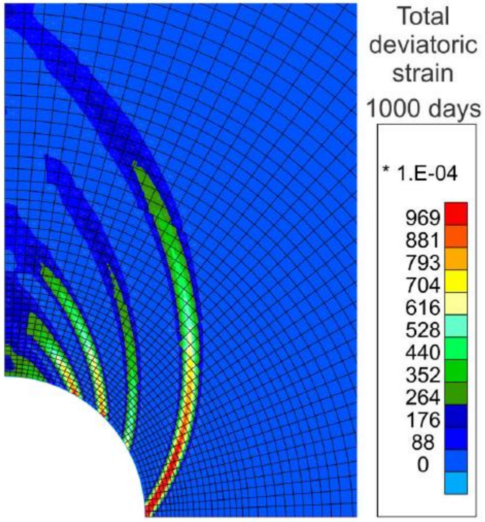

Gallery ventilation :

Pressure at gallery wall :

→ gallery excavation : σ_x and σ_y decrease

→ gallery ventilation : water phases equilibrium (Kelvin's law) $RH = \frac{p_v}{p_{v,0}} = exp\left(\frac{-p_c M_v}{RT \rho_w}\right)$

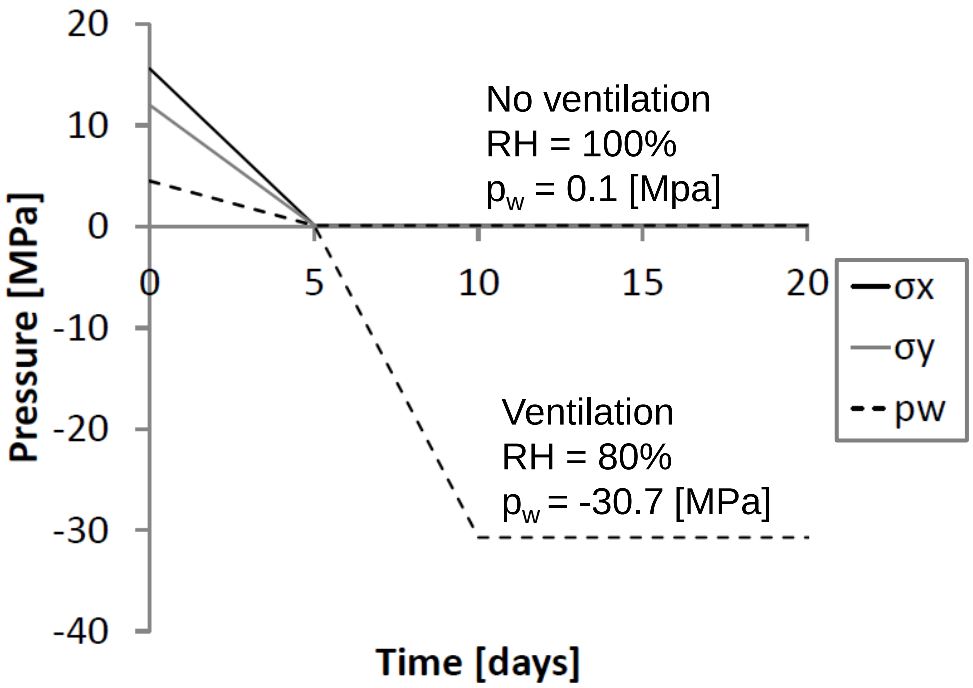

Influence of gallery ventilation :

End of excavation ↓ | No ventilation

3 days | 4 days | 5 days | 100 days | 1000 days

Total deviatoric strain

0 0.184

Plasticity

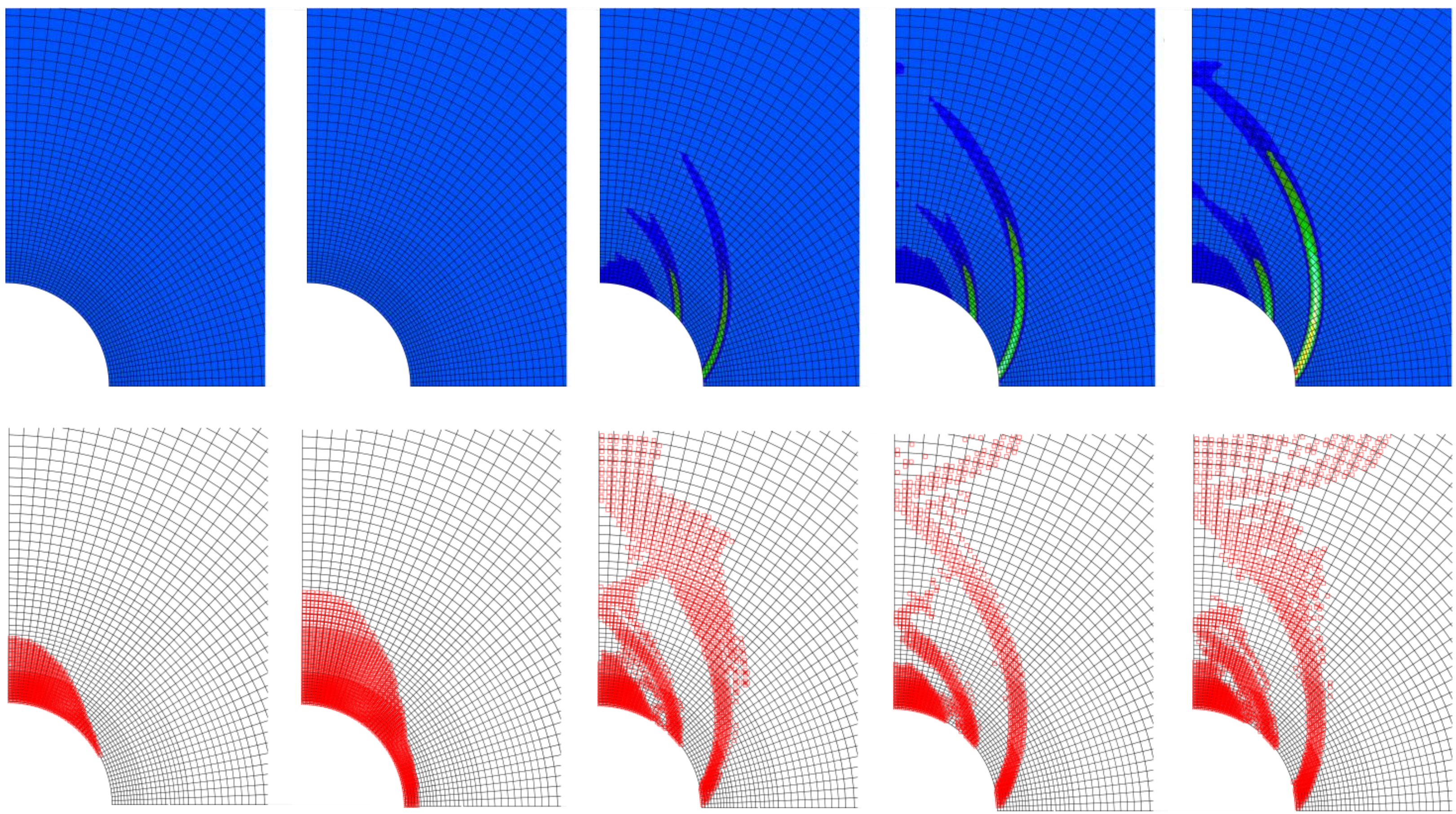

2. Numerical results for gallery excavation – 2D

Influence of gallery ventilation :

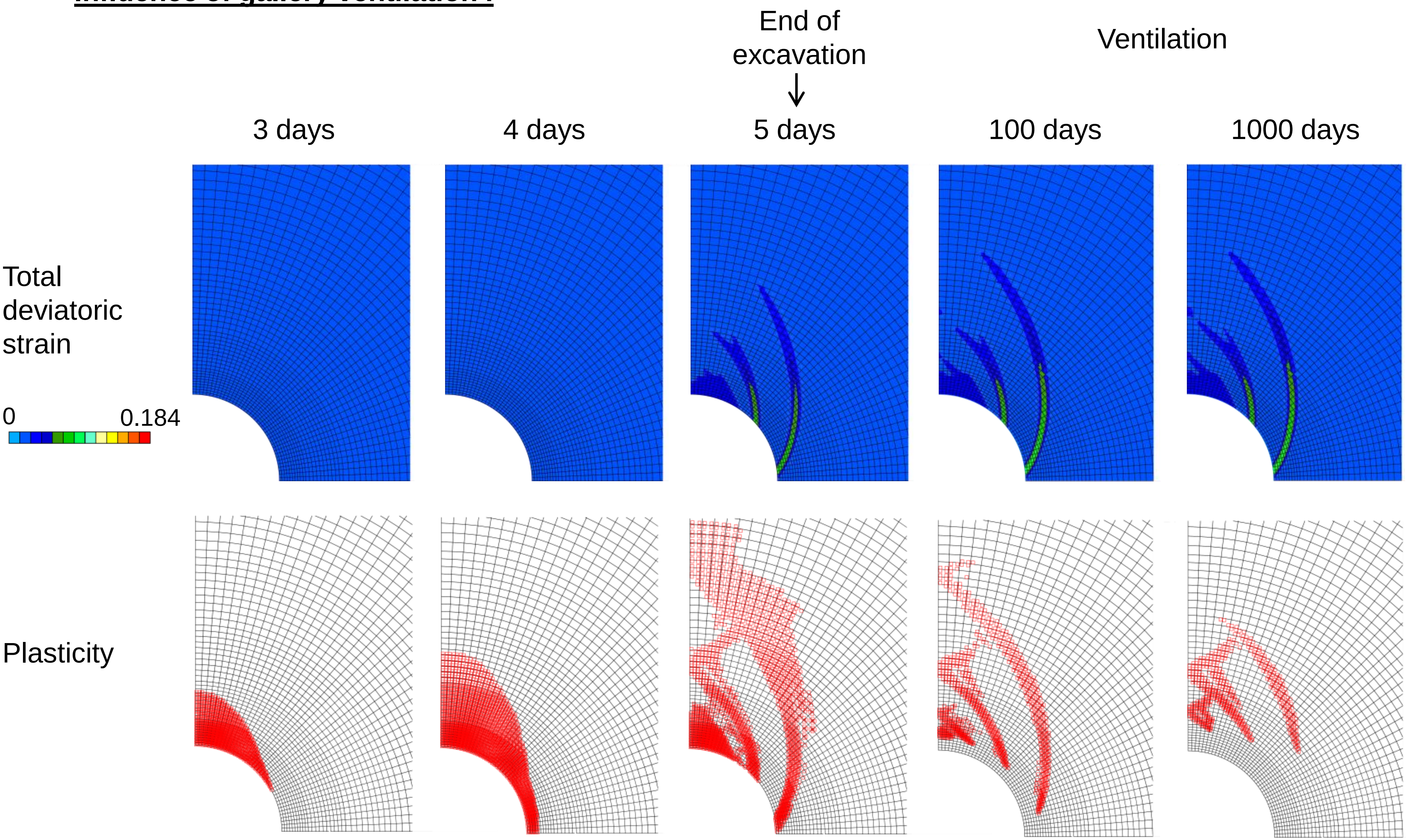

Influence of gallery ventilation : No ventilation

Cross-section

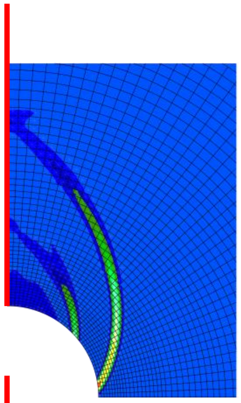

Pore water pressure

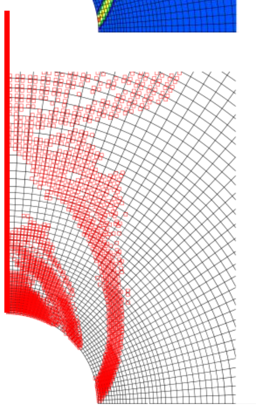

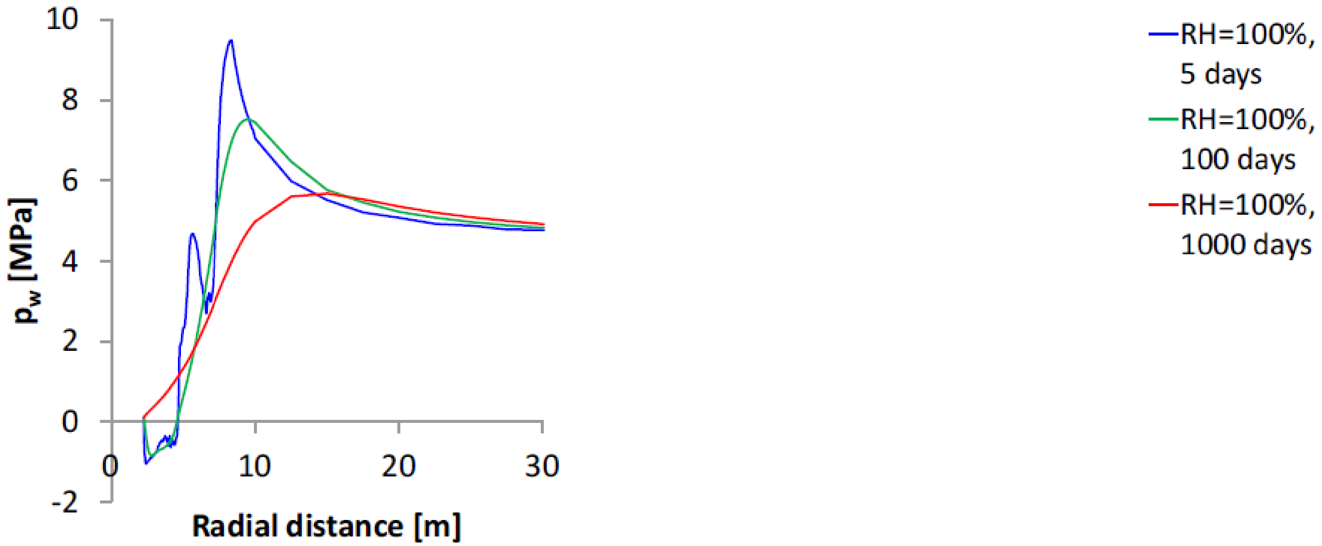

2. Numerical results for gallery excavation – 2D

<u>Influence of gallery ventilation :</u> No ventilation

Cross-section

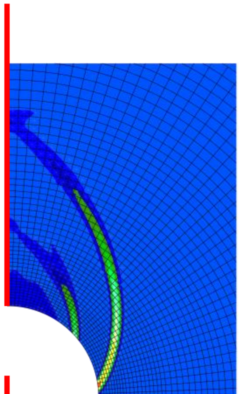

Pore water pressure

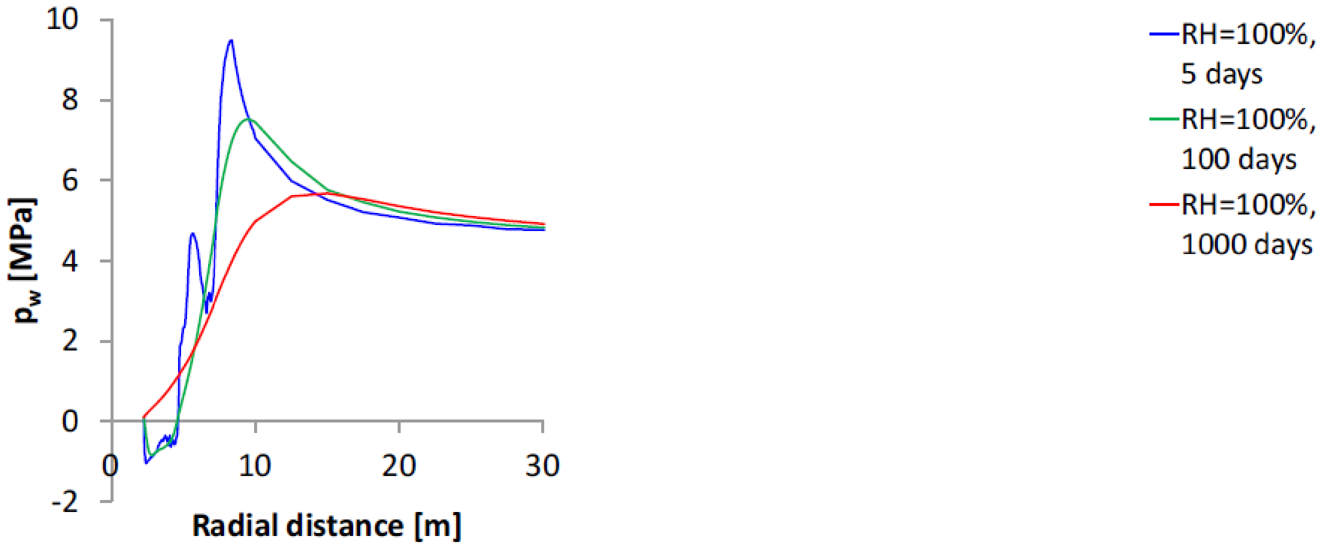

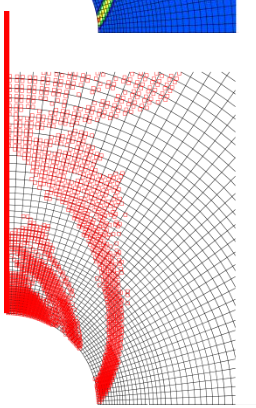

Degree of saturation

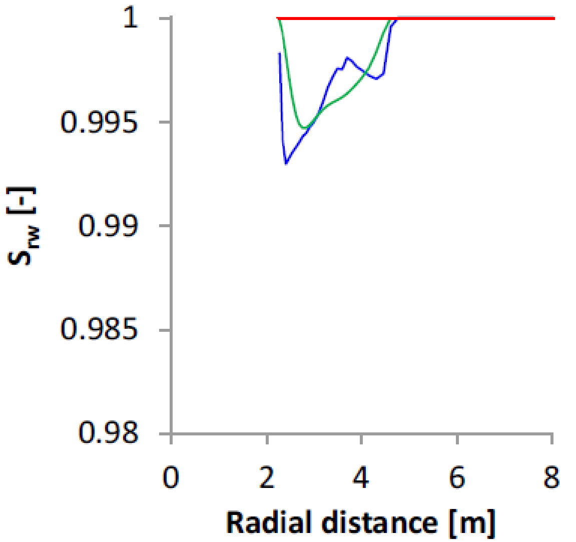

Influence of gallery ventilation :

No ventilation

Ventilation

Cross-section

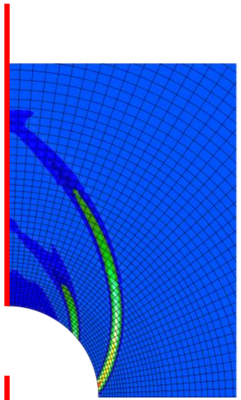

Pore water pressure

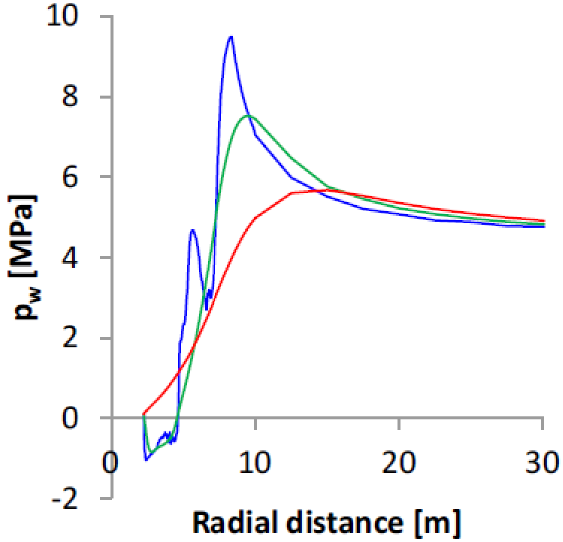

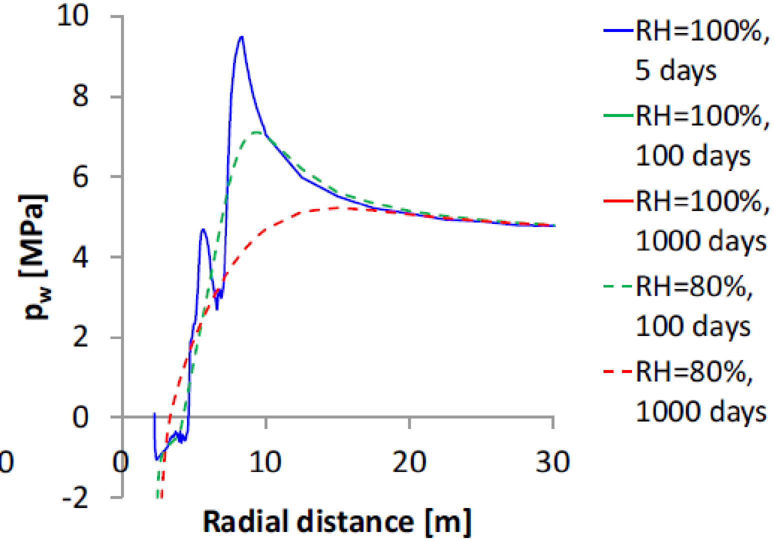

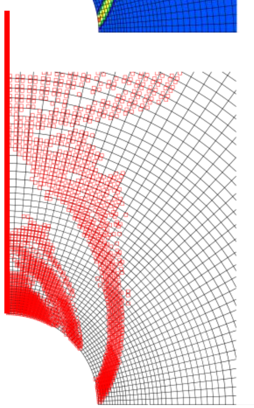

Degree of saturation

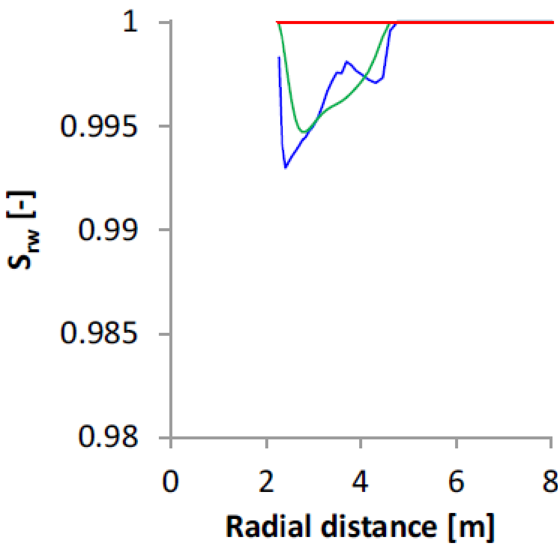

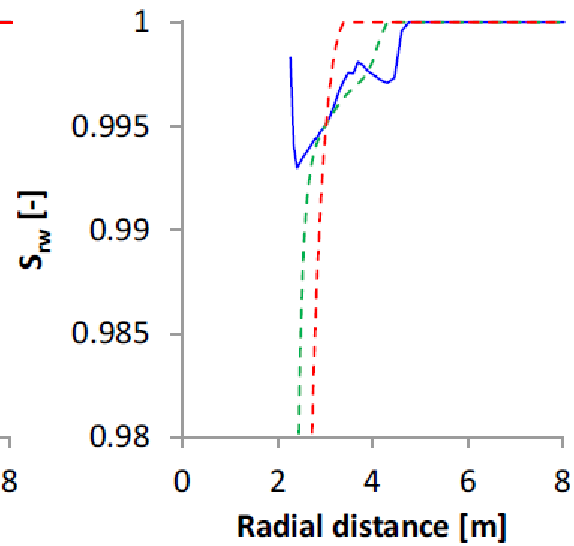

Influence of gallery ventilation :

Convergence

Vertical

Horizontal

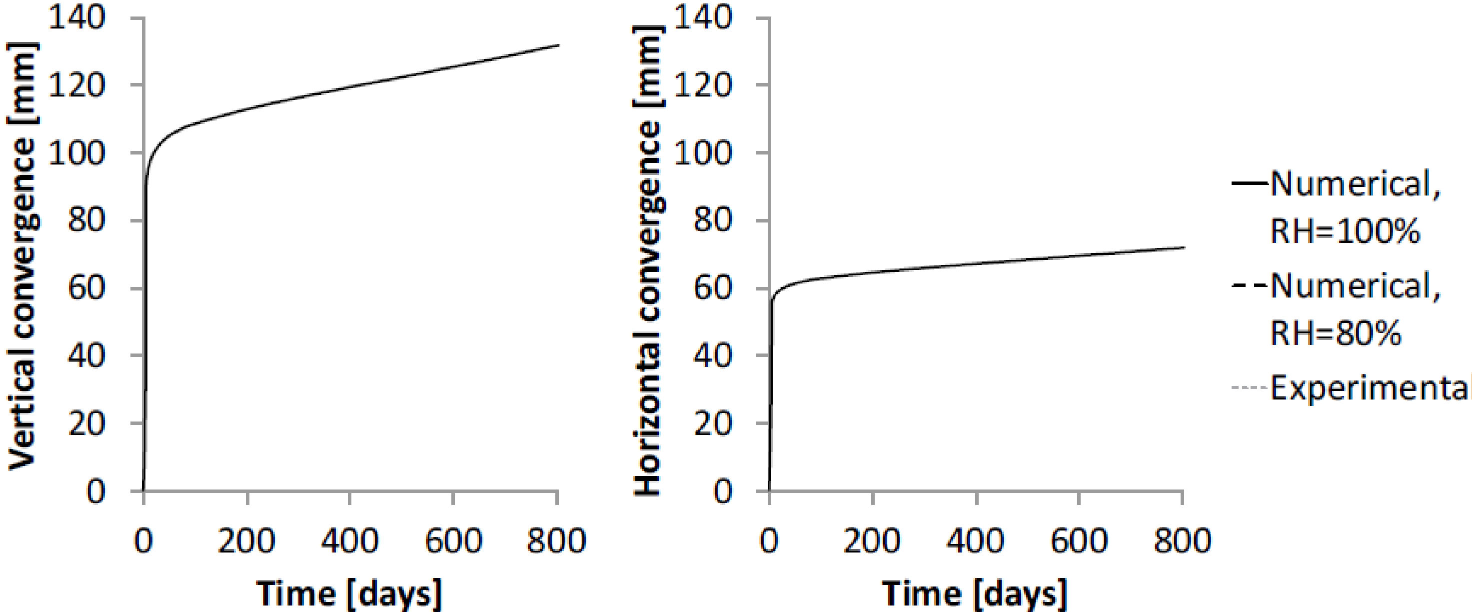

ventilation

Important during the excavation and keeps increasing afterwards.

Anisotropic convergence because of the shear strain localisation bands located above the gallery.

Influence of gallery ventilation :

Convergence

Vertical Horizontal

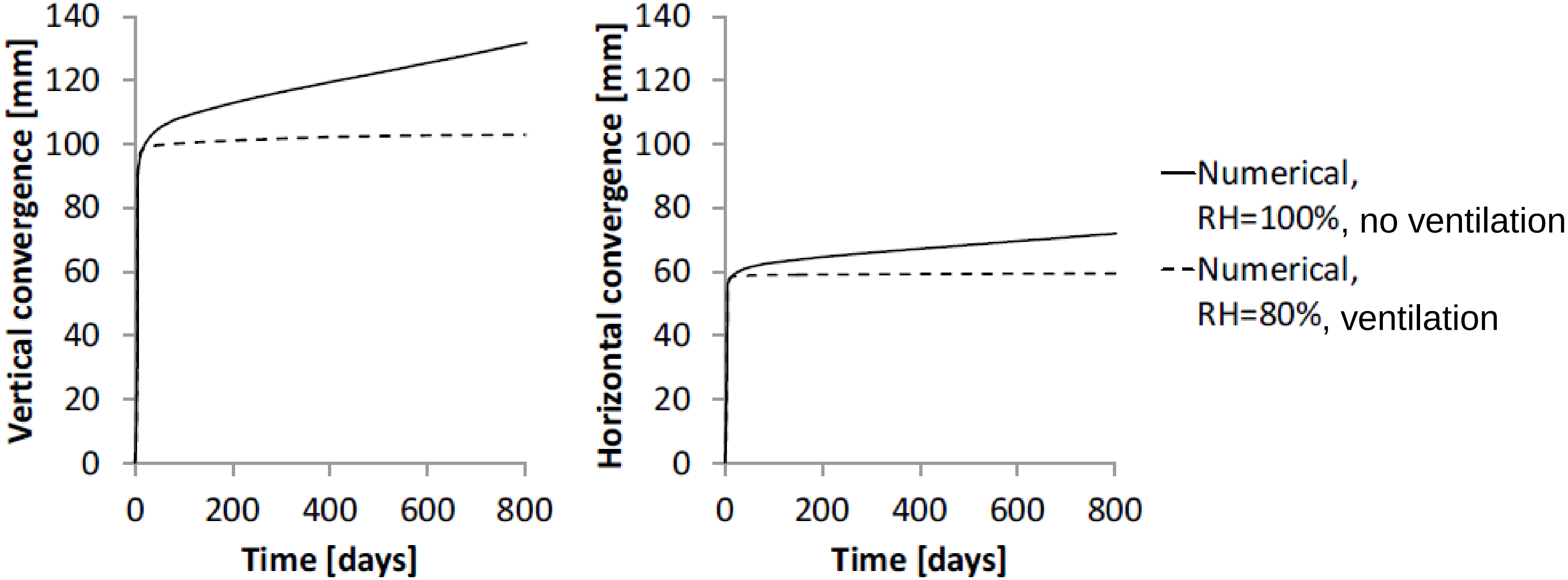

Important during the excavation and keeps increasing afterwards.

Anisotropic convergence because of the shear strain localisation bands located above the gallery.

Influence of the ventilation.

Influence of gallery ventilation :

Convergence

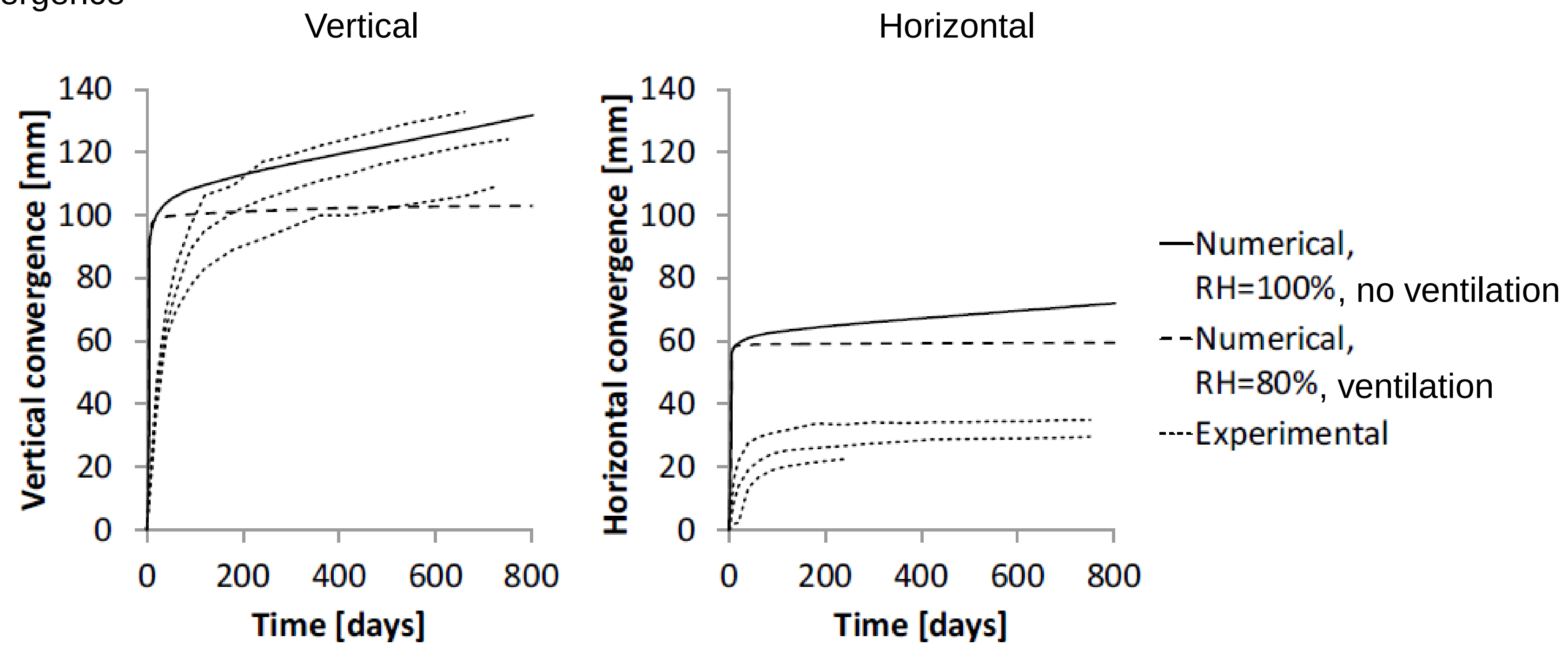

Important during the excavation and keeps increasing afterwards.

Anisotropic convergence because of the shear strain localisation bands located above the gallery.

Influence of the ventilation.

Experimental results from a gallery of the Andra URL (Armand *et al.* 2013, Cruchaudet *et al.*, 2010b).
Good matching in the vertical direction for the modelling without ventilation.

2. Numerical results for gallery excavation – 2D

Permeability variation :

Hydraulic properties is not homogeneous in the damaged zone.

Influence of rock fracturing on intrinsic permeability.

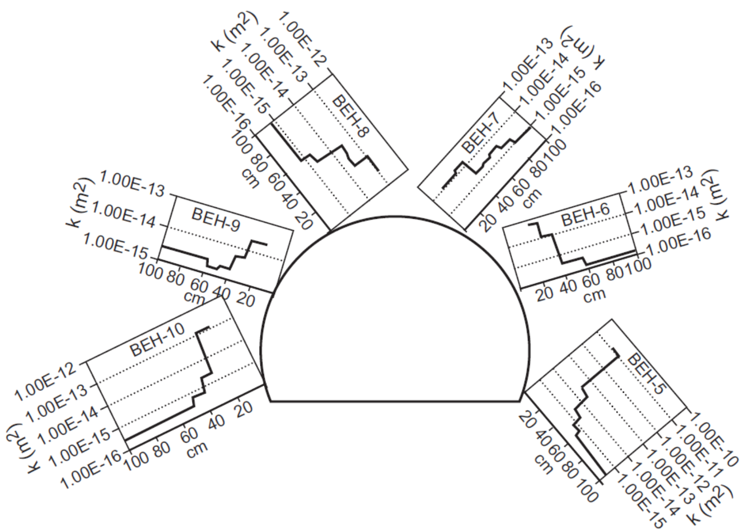

Permeability increase in Opalinus clay
(Bossart et al., 2002)

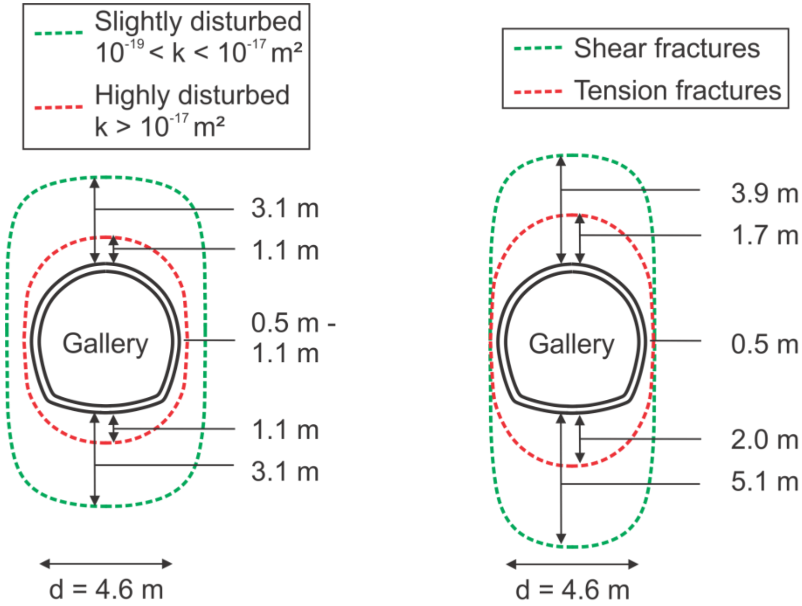

In situ permeability and fractures in Callovo-Oxfordian claystone (Armand *et al.* 2013, Cruchaudet *et al.* 2010b)

Permeability variation :

Cubic evolution of k with **porosity** :

$$\frac{k_{ij}}{k_{ij,0}} = 1 + \alpha (n - n_0)^{\beta}$$

$\alpha = 2 \times 10^{12}$, $\beta = 3$

End of excavation

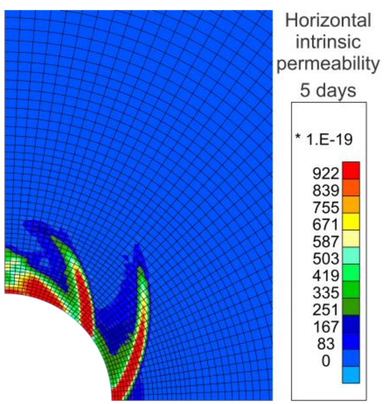

Vertical cross-section

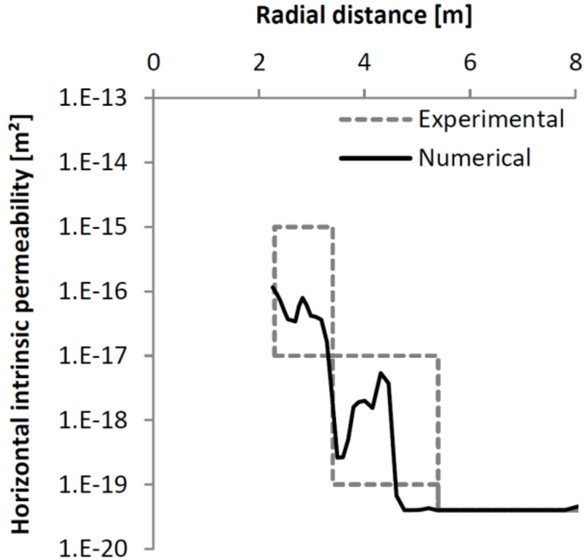

Horizontal cross-section

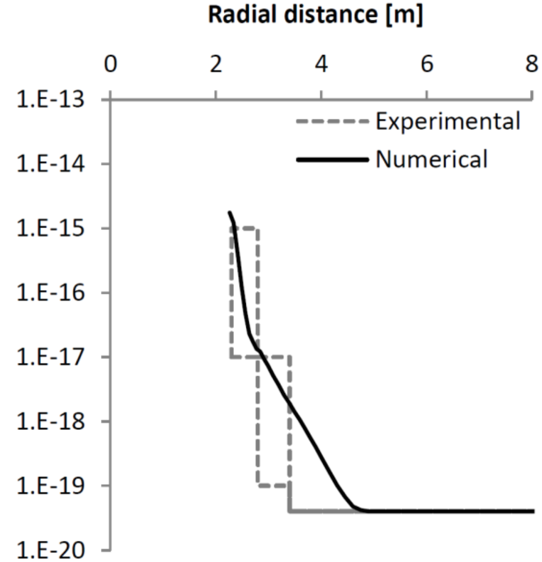

Permeability variation :

Cubic evolution of k with **total equivalent strain** :

$$\frac{k_{ij}}{k_{ij,0}} = 1 + \alpha(\varepsilon_{eq} - 0.01)^{\beta} \qquad \text{if } \varepsilon_{eq} > 0.01$$

$\alpha = 2 \times 10^8$, $\beta = 3$

$$\varepsilon_{eq} = \sqrt{\frac{3}{2}\hat{\varepsilon}_{ij}\hat{\varepsilon}_{ij}} \qquad \hat{\varepsilon}_{ij} = \varepsilon_{ij} - \varepsilon_m \delta_{ij}$$

End of excavation

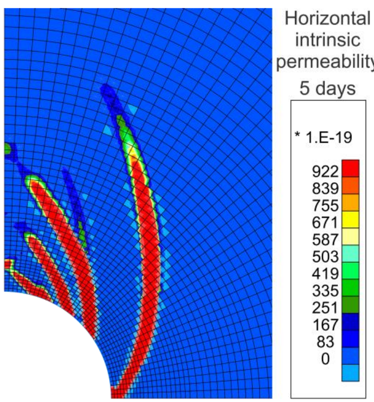

Vertical cross-section

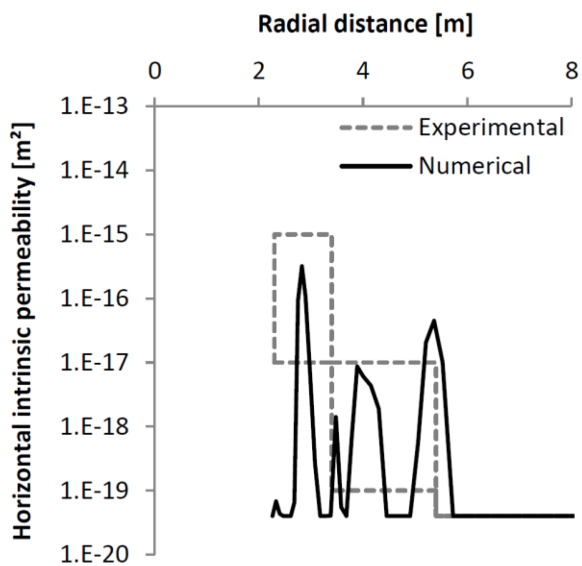

Horizontal cross-section

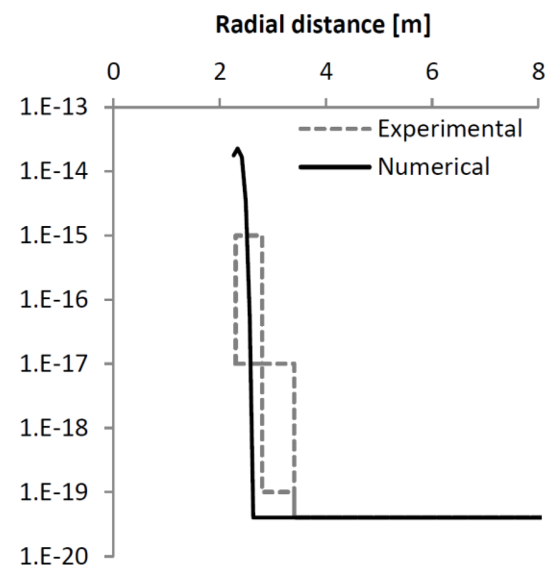

<u>Permeability variation :</u> **Pore water pressure, influence of ventilation**

5 days
End of excavation

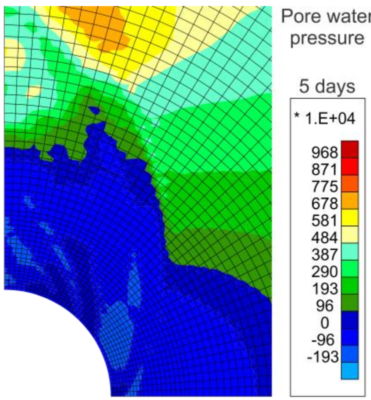

1000 days
End of calculation

No ventilation (RH=100%)

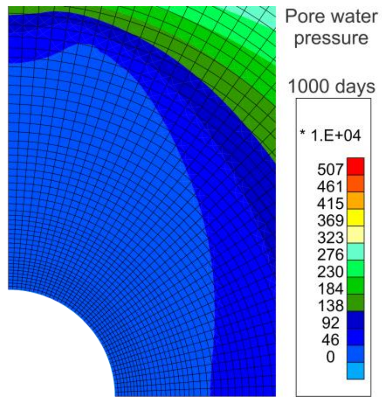

1000 days
End of calculation

Ventilation (RH=80%)

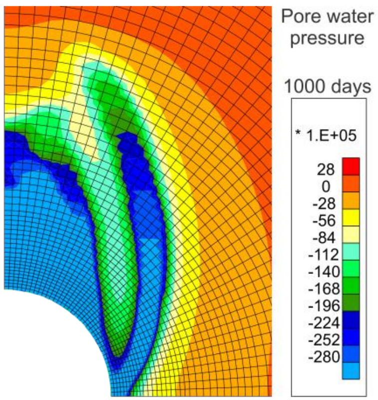

Permeability variation :

Pore water pressure, influence of ventilation

5 days
End of excavation

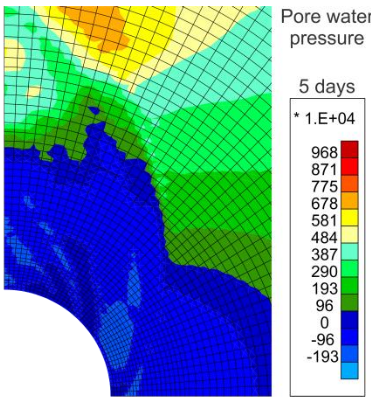

1000 days
End of calculation

No ventilation (RH=100%)

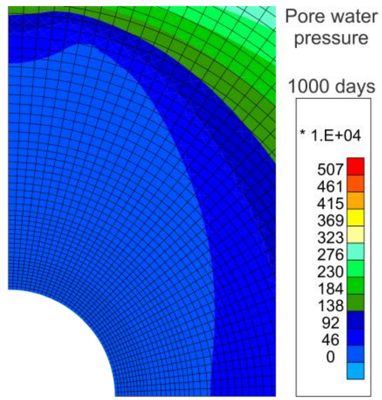

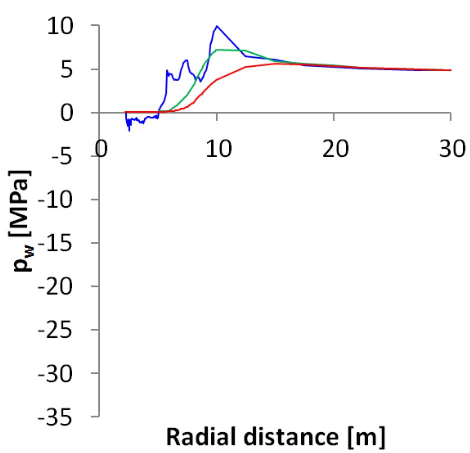

1000 days
End of calculation

Ventilation (RH=80%)

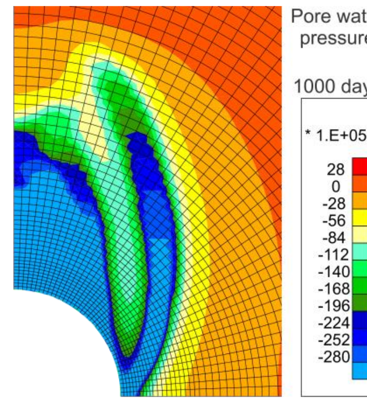

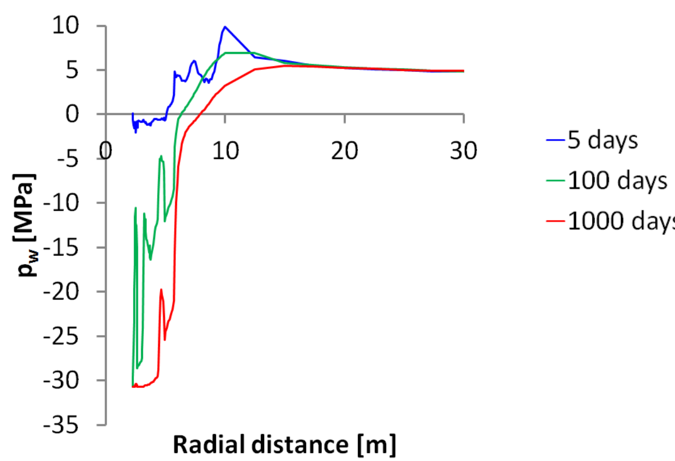

Vertical
cross-section

Permeability variation :

Pore water pressure, influence of ventilation and permeability variation

No ventilation (RH=100%) | Ventilation (RH=80%)

Vertical cross-section

k = cst

Vertical cross-section

k = f(ε_{eq})

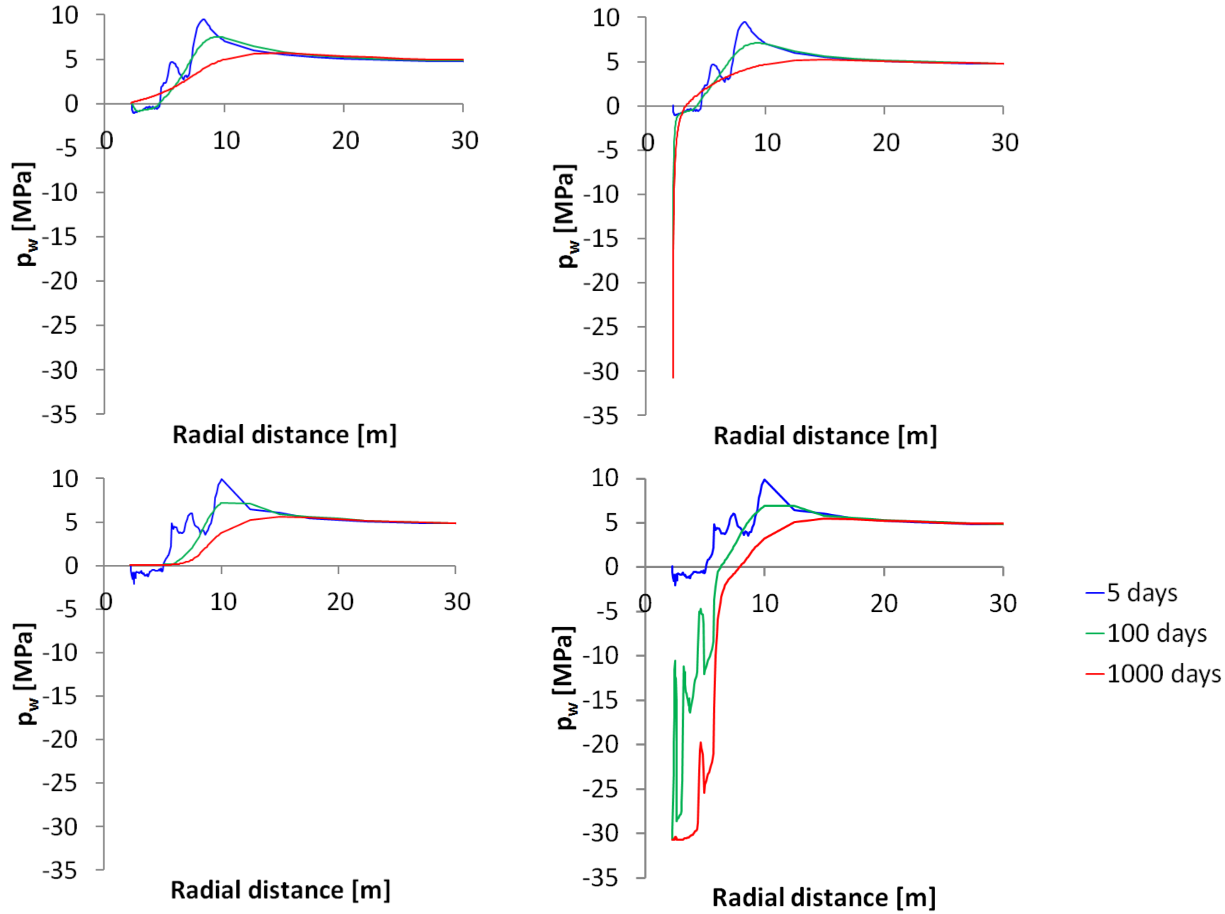

Outline

1. CONSTITUTIVE MODELS

2. **NUMERICAL RESULTS FOR GALLERY EXCAVATION**

   - 2D : ventilation, permeability variation

   - **3D**

3. CONCLUSIONS AND OUTLOOKS

2. Numerical results for gallery excavation – 3D

Numerical modelling (LAGAMINE-ULg) :

Mechanical modelling in 3D state.
Classical FE, no second gradient !

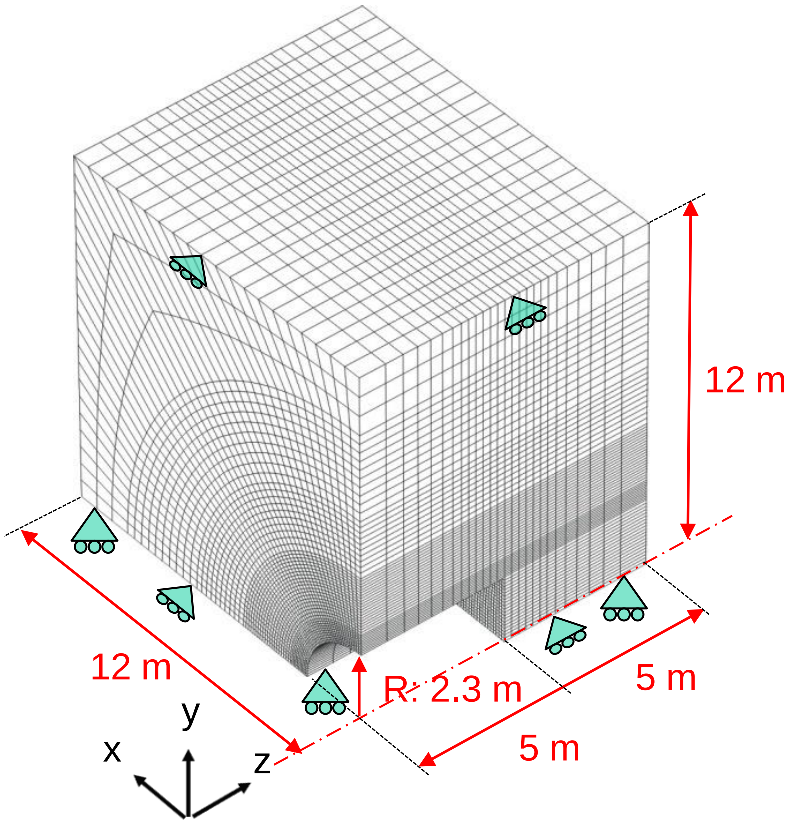

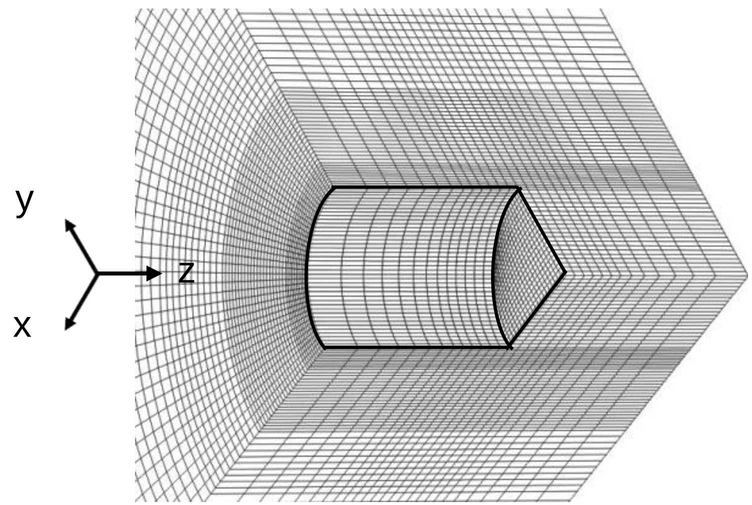

Numerical modelling (LAGAMINE-ULg) :

Mechanical modelling in 3D state.
Classical FE, no second gradient !

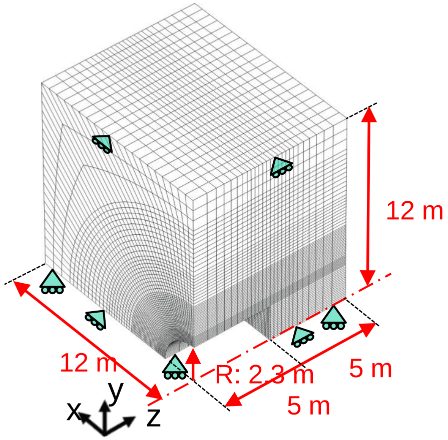

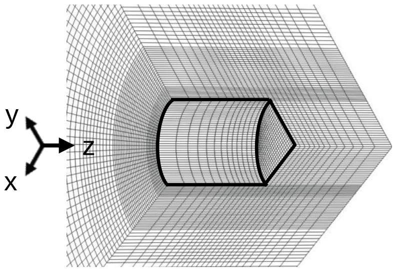

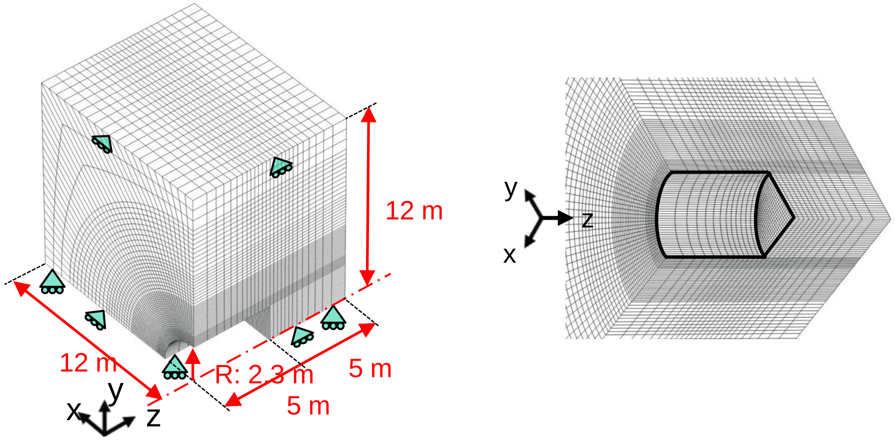

Numerical modelling (LAGAMINE-ULg) :

Mechanical modelling in 3D state.
Classical FE, no second gradient !

Localisation zone :

Equivalent deformation ε_{eq} - during boring

3 days	3.25 days	3.5 days	3.75 days	4 days	4.25 days
$\sigma/\sigma_0 = 0.40$	$\sigma/\sigma_0 = 0.35$	$\sigma/\sigma_0 = 0.30$	$\sigma/\sigma_0 = 0.25$	$\sigma/\sigma_0 = 0.20$	$\sigma/\sigma_0 = 0.15$

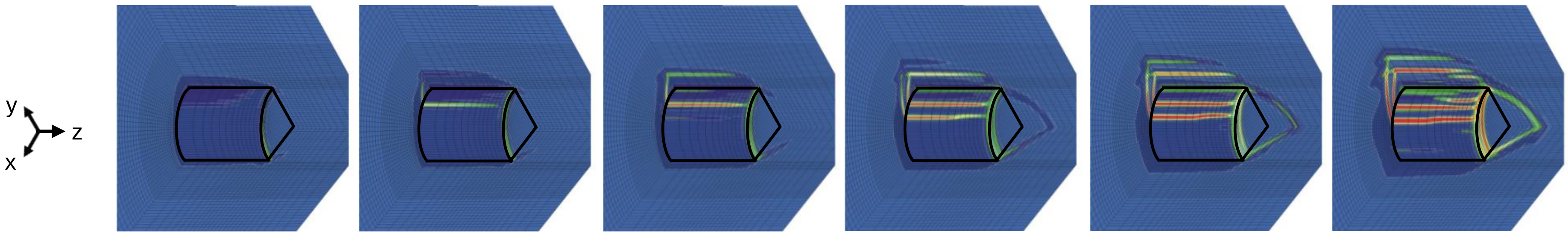

Numerical modelling (LAGAMINE-ULg) :

Mechanical modelling in 3D state.
Classical FE, no second gradient !

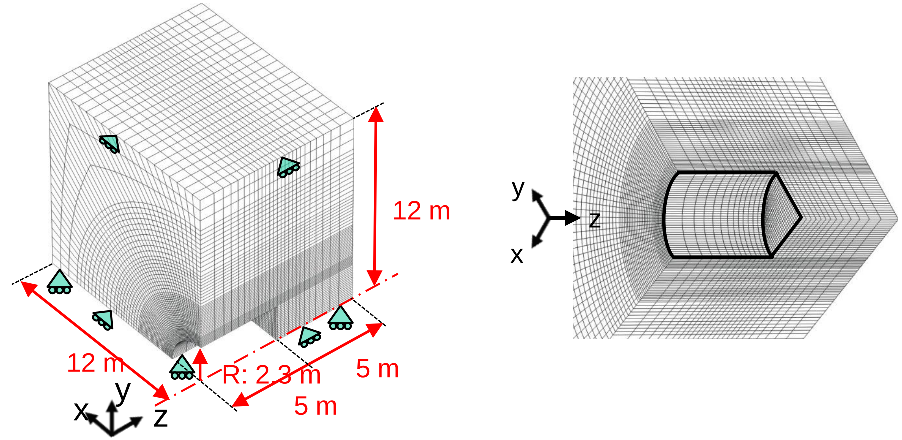

Localisation zone :

Equivalent deformation ε_{eq} - during boring

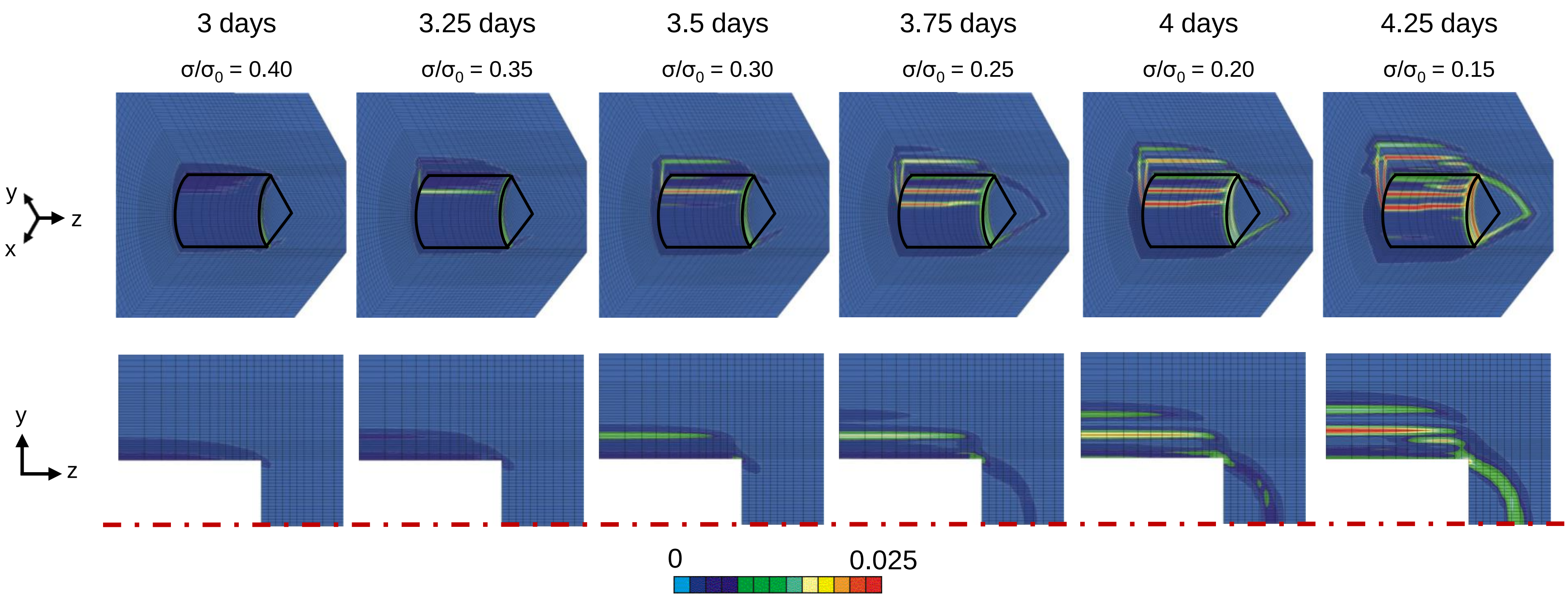

<u>Localisation zone :</u> Equivalent deformation ε_{eq} - for 4.25 days of excavation ($\sigma/\sigma_0 = 0.15$) :

z<0 : excavation zone
z=0 : gallery front
z>0 : rock mass

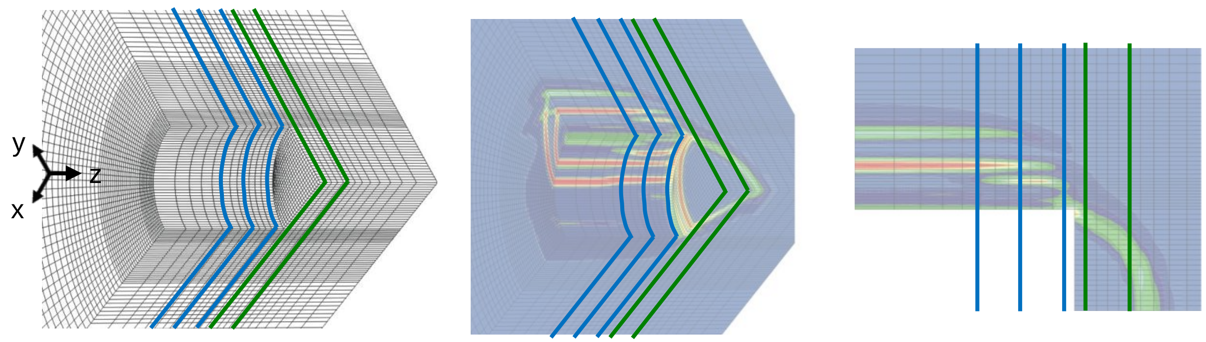

z=-2.25m z=-1.25m z=-0.25m z=+0.25m z=+1.25m

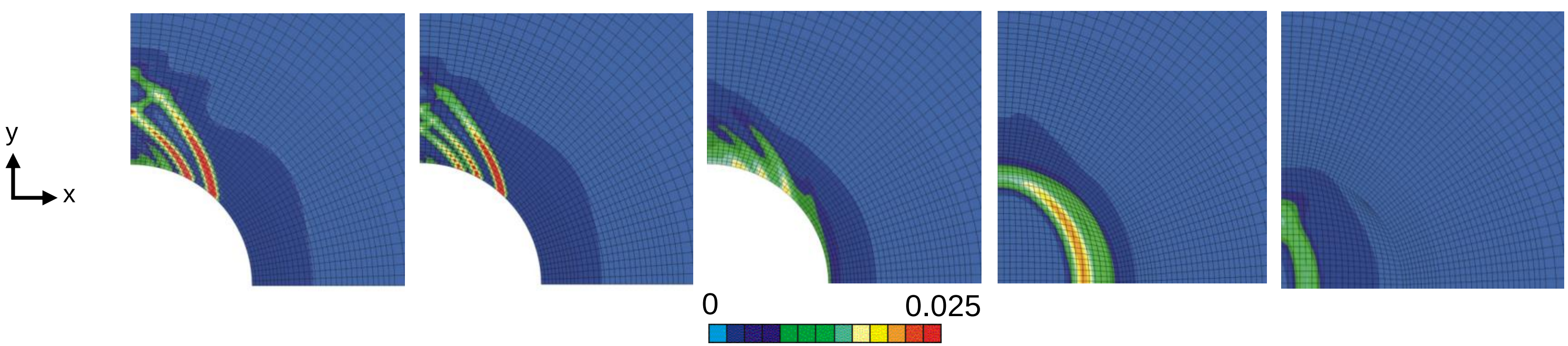

Localisation zone : Equivalent deformation ε_{eq} - for 4.25 days of excavation ($\sigma/\sigma_0 = 0.15$) :

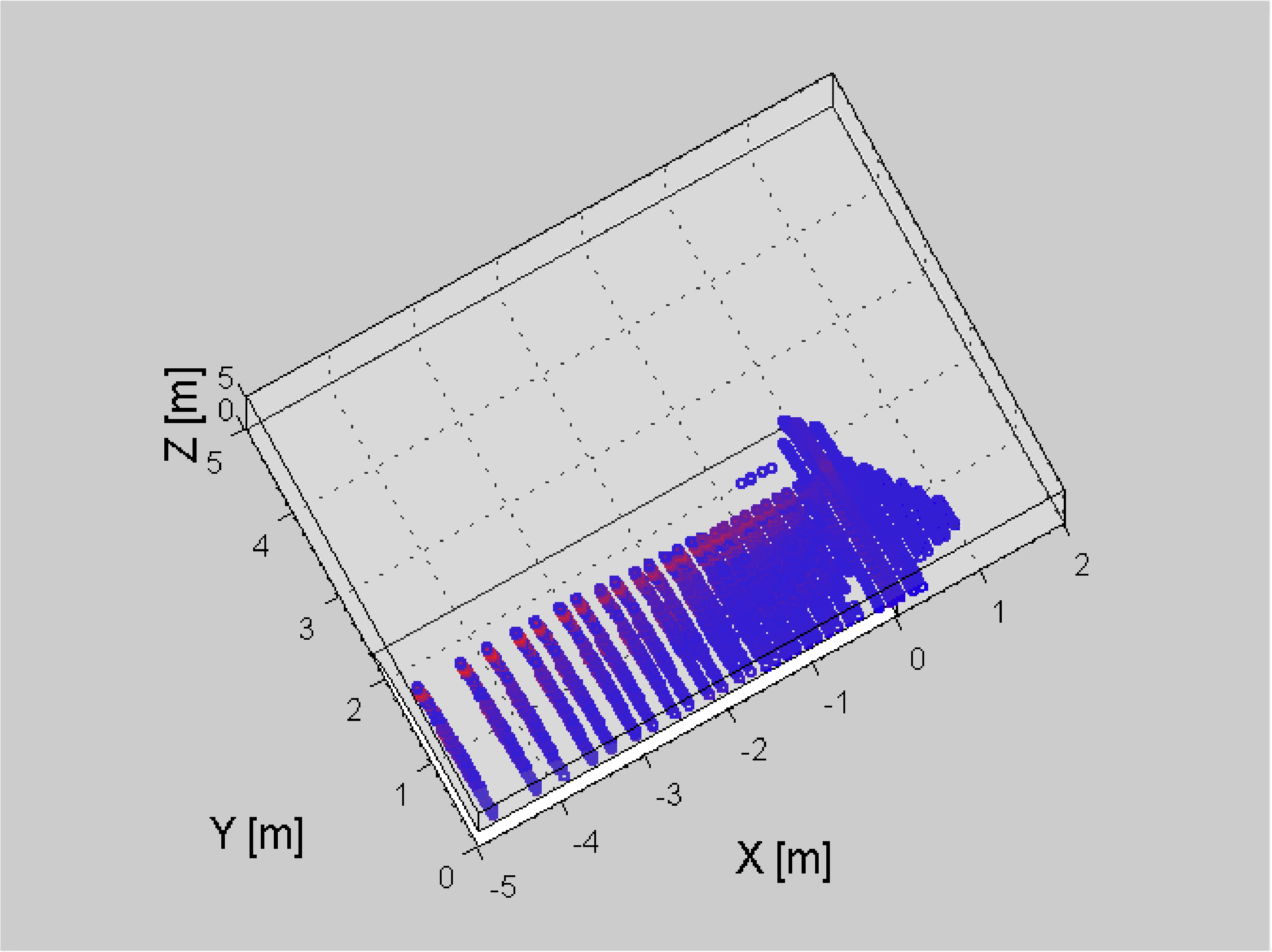

Outline

Damaged zone → strain localisation zone similar to *in situ* measurements

→ modelling provide information about the rock structure and evolution within this zone, as observed *in situ*.

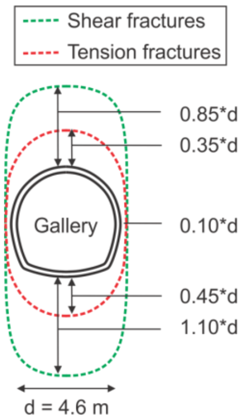

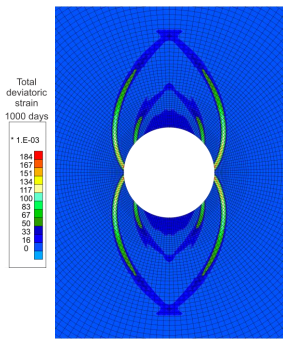

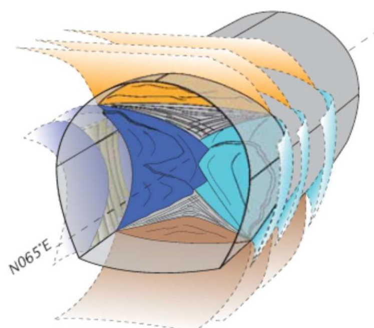

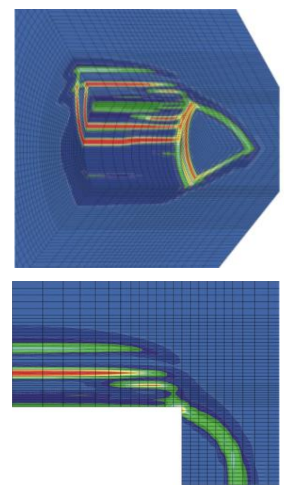

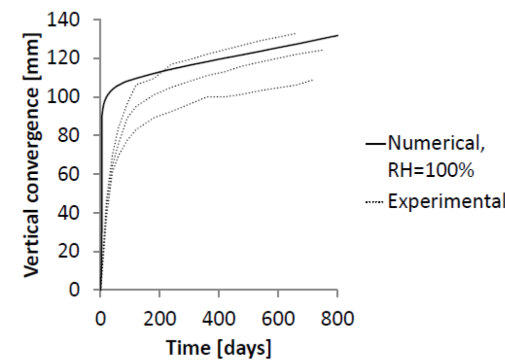

.

→ need for a <u>better definition of :</u>

<u>- the rock anisotropy</u>

<u>- the properties changes</u>

<u>- the hydromechanical coupling</u>

APPENDIX

References

Armand G.,Leveau F., Nussbaum C., de La Vaissiere R., Noiret A., Jaeggi D., Landrein P.,Righini C. “Geometry and properties of the excavation induced fractures at the Meuse/Haute-Marne URL drifts”, Rock Mechanics and Rock Engineering, 2013.

Bossart P., Meier P. M., Moeri A., Trick T., Mayor J.C., “Geological and hydraulic characterisation of the excavation disturbed zone in the Opalinus Clay of the Mont Terri Rock Laboratory”, Engineering Geology, vol. 66, n° 1-2, 2002, p. 19–38.

Chambon R., Caillerie D., El Hassan N., “One-dimensional localisation studied with a second grade model”, European Journal of Mechanics - A/Solids, vol. 17, n° 4, 1998, p. 637–656.

Chambon R., Caillerie D., Matsushima T., “Plastic continuum with microstructure, local second gradient theories for geomaterials : localization studies”, International Journal of Solids and Structures, vol. 38, 2001, p. 8503-8527.

Chambon R., Crochepeyre S., Charlier R., “An algorithm and a method to search bifurcation points in non-linear problems”, International Journal for Numerical Methods in Engineering, vol. 51, 2001, p. 315–332.

Charlier R., Collin F., Pardoen B., Talandier J., Radu JP., Gerard P., “An unsaturated hydro-mechanical modelling of two in-situ experiments in callovo-oxfordian argillite”. Engineering Geology, 2013, in press.

Collin F., Chambon R., Charlier R., “ A finite element method for poro mechanical modelling of geotechnical problems using local second gradient models”, International Journal for Numerical Methods in Engineering, vol. 65, n° 11, 2006, p. 1749–1772.

Cruchaudet M., Noiret A., Talandier J., Gatmiri B., Armand G., “OHZ en GED : EDZ initiale et évolution”, rapport interne n° D.RP.AMFS.11.0016, 2010b, ANDRA.

Germain P., “The method of virtual power in continuum mechanics. Part 2 Microstructure”, SIAM Journal on Applied Mathematics, vol. 25, 1973, p. 556-575.

Mindlin R.D., “Micro-structure in linear elasticity”, Archive for Rational Mechanics and Analysis, vol. 16, 1964, p. 51–78.

Sieffert Y., Al Holo S., Chambon R., "Loss of uniqueness of numerical solutions of the borehole problem modelled with enhanced media", International Journal of Solids and Structures, vol. 46, 2009, p. 3173–3197.

Toupin R., “Elastic materials with couple–stresses”, Archive for Rational Mechanics and Analysis, vol. 11, 1962, p. 385–414.

Zervos A., Papanastasiou P., Vardoulakis I., “Modelling of localisation and scale effect in thick-walled cylinders with gradient elastoplasticity”, International Journal of Solids and Structures, vol. 38, 2001, p. 5081-5095.

Mechanical and hydraulic parameters :

Synthesis of Callovo-Oxfordian claystone parameters from (Charlier et al. 2013 in press)

Symbol	Name	Value	Unit
k_{hor}	Horizontal intrinsic water permeability	4 10^{-20}	m²
k_{vert}	Vertical intrinsic water permeability	1.33 10^{-20}	m²
n_0	Porosity	0.18	-
M	Van Genuchten coefficient	0.33	-
N	Van Genuchten coefficient	1.49	MPa
P_r	Van Genuchten parameter	15	Pa^{-1}

Permeability anisotropy

Symbol	Name	Value	Unit
E	Young's modulus	4000	MPa
ν	Poisson's ratio	0.3	-
b	Biot's coefficient	0.6	-
ρ_s	Specific mass	2300	kg/m³
ψ	Dilatancy angle	0.5	°
φ_0	Initial friction angle	10	°
φ_f	Final friction angle	20	°
B_φ	Friction angle hardening coefficient	0.002	-
c_0	Initial cohesion	3	MPa
c_f	Final cohesion	0.3	MPa
B_c	Cohesion softening coefficient	0.003	-
D	Second gradient elastic parameter	5000	N

Friction angle hardening

Cohesion softening